

AMERICAN UNIVERSITY OF BEIRUT

OCCURRENCE AND TRANSPORT OF SELECTED
MICROPOLLUTANTS IN SURFACE WATER AND
GROUNDWATER UNDER VARYING DYNAMIC CONDITIONS:
APPLICATION ON THE QACHQOUCH KARST CATCHMENT-
LEBANON

by
MICHEL ELIE AOUN

A thesis
submitted in partial fulfillment of the requirements
for the degree of Master of Science
to the Department of Geology
of the Faculty of Arts and Sciences
at the American University of Beirut

Beirut, Lebanon
December 2019

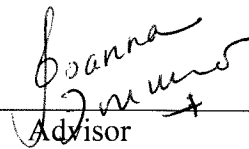
AMERICAN UNIVERSITY OF BEIRUT

OCCURRENCE AND TRANSPORT OF SELECTED
MICROPOLLUTANTS IN SURFACE WATER AND
GROUNDWATER UNDER VARYING DYNAMIC CONDITIONS:
APPLICATION ON THE QACHQOUCH KARST CATCHMENT-
LEBANON

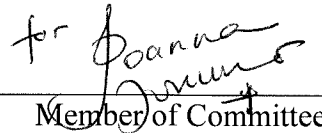
by
MICHEL ELIE AOUN

Approved by:

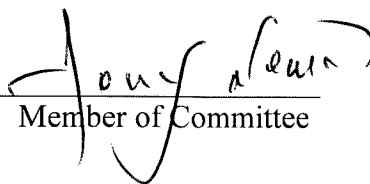
Dr. Joanna Doummar, Assistant Professor
Geology


Advisor

Dr. Josep Sanjuan Girbau, Assistant Professor
Geology


Member of Committee

Dr. Tony Nemer, Assistant Professor
Geology


Member of Committee

Date of thesis defense: December 23, 2019

AMERICAN UNIVERSITY OF BEIRUT

THESIS, DISSERTATION, PROJECT RELEASE FORM

Student Name: Michel Elie Aoun

Master's Thesis
Dissertation

Master's Project

Doctoral



I authorize the American University of Beirut to: (a) reproduce hard or electronic copies of my thesis, dissertation, or project; (b) include such copies in the archives and digital repositories of the University; and (c) make freely available such copies to third parties for research or educational purposes.



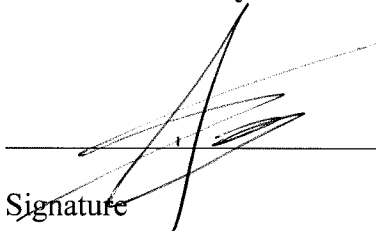
I authorize the American University of Beirut, to: (a) reproduce hard or electronic copies of it; (b) include such copies in the archives and digital repositories of the University; and (c) make freely available such copies to third parties for research or educational purposes after : **One ---- year from the date of submission of my thesis, dissertation, or project.**

Two ---- years from the date of submission of my thesis, dissertation, or project.

Three ---- years from the date of submission of my thesis, dissertation, or project.

Signature

Date



19/Feb/2020

ACKNOWLEDGMENTS

I would like to express my sincere gratitude to my advisor, Dr. Joanna Doummar for the continuous support, motivation, guidance, enthusiasm, patience, and empathy. I appreciate her outstanding research intellect, immense knowledge, and her wonderful personality.

“Imagine smiling after a slap in the face. Then think of doing it twenty-four hours a day.”

Markus Zusak

Dedicated to the memory of my mother, Maya, who was an academic, and taught me everything I know. The toughest lessons you taught me came after your passing.

You are gone, but your belief in me kept me going and rising.

Table of Contents

Acknowledgments.....	4
An Abstract of the thesis.....	9
1. Chapter 1 - Introduction.....	10
2. Chapter 2 - Background Studies.....	12
2.3.1 Artificial tracers and experiments.....	16
2.3.1.1 Applications of tracer tests.....	16
2.3.1.2 Interpretation of tracer tests.....	17
2.3.1.3 Analytical models of transport parameters.....	21
2.3.2 Natural tracers: stable isotopes.....	22
2.3.3 Spring chemograph and hydrograph analyses.....	23
2.3.4 Micropollutants.....	24
3. Chapter 3- Field Site.....	31
4. Chapter 4 - Methods.....	38
4.1.1 Spring monitoring.....	38
4.1.2 Physico-chemical and bacteriological sampling.....	39
4.1.3 Micropollutant sample collection.....	40
4.1.4 Artificial tracer experiments.....	41
4.1.5 Discharge measurement.....	42
4.2.1 Physico-chemical and bacterial analyses.....	43
4.2.2 Micropollutant analyses.....	45
4.3.1 Modeling of tracer breakthrough curves.....	45
4.3.2 Discharge.....	46
4.3.3 Origin of inflowing water.....	48
4.3.4 Quantification of volume of new waters.....	49
4.3.5 Estimation of recharge altitude based on isotopic signature.....	50
4.3.6 Standard deviations and regression analysis.....	50
4.3.7 Calculation of number of inhabitants using specific medical products.....	51
5. Chapter 5 - Results.....	52
5.1.1 Nahr el Kalb River.....	52
5.1.2 Qachqouch Spring.....	52
5.2.1 Campaign 1: 2015.....	55
5.2.2 Campaign 2: 2017.....	59
6. Chapter 6 - Discussion.....	71
7. Chapter 7 - Conclusion.....	82
8. Chapter 8 - References.....	85

1. AN ABSTRACT OF THE THESIS OF

Michel Elie Aoun for Master of Science
Major: Geology

Title: Occurrence and transport of selected micropollutants in surface water and groundwater under varying dynamic conditions: Application on the Qachqouch karst catchment – Lebanon.

The occurrence of specific micropollutants (MPs), indicators of domestic and hospital wastewater, was investigated in this specific River based on two sampling campaigns under varying flow conditions. The MPs characterized by a high frequency of occurrence; Acesulfame-K (ACE-K), Ibuprofen (IBU), Gemfibrozil (GEM), Nonylphenol (NON), and Iohexol (IOX) were highly reflective of wastewater discharged in ephemeral streams and tributaries, as well as specific point sources such as farms and hospital effluents. A mixing model based on chloride mass fluxes allows the quantification of the percentage of untreated wastewater effluents in inflowing water from river tributaries, which varied between 0.7-99 % and 5.0-10 % in low flow and high flow respectively. The frequency of occurrence of MPs is related to the volume of wastewater input, extent of river dilution, persistence of the MPs, and type of point source contamination on the River. Relationships were established between MPs such as IBU and ACE-K, indicating their co-existence in highly consumed generic medicine and their suitability as wastewater co-tracers. Multiple artificial tracer experiments showed that Nahr El Kalb River is connected to the Qachqouch spring through a point source sinking stream.

A detailed analysis of selected spring responses' chemograph and hydrograph following a multi precipitation event shows that three of the tracked MPs, especially ACE-K, and to the exception of IOX, can be used as specific indicators for point source domestic wastewater in karst systems. They have revealed to be persistent, source specific, conservative, and highly correlated with in-situ parameters easily measurable at the spring (chloride and turbidity). Even if the selected MPs are found in the system during low flow periods, they are mostly transported to the spring through fast flow pathways from flushed wastewater with surface water or flood rainwater. The highest mass inflow of ACE-K, IOX and GEM originated from a sinking stream, while SUC infiltrated exclusively through fast infiltration points (dolines). Their breakthrough curves coincide with the arrival of new waters and turbidity peaks. Unlike IOX, the mass fluxes of ASWs, and GEM to a lesser extent, can be used as indicators as they are linearly correlated with chloride mass fluxes and turbidity flux.

CHAPTER

1. INTRODUCTION

Karst aquifers supply about 25% of the world population, and in some European countries even 50% with drinking water (Ford and Williams, 2007), especially in Mediterranean semi-arid regions. The sensitivity of karst systems for contamination is difficult to assess due to their duality of infiltration and flow. On the one hand, they are recharged through concentrated infiltration in dolines and/or dry valleys. On the other hand, diffuse recharge also occurs through soil and epikarst forming a relatively thick unsaturated zone (Geyer et al., 2008; Perrin et al., 2003). A duality of flow is observed in the saturated zone, where a conduit system is draining low permeability matrix storage (Doummar et al., 2012; Geyer et al., 2007; Király, 2002). Essentially, due to heterogeneities, vulnerability in karst aquifers is controversial especially when compared to porous aquifers (Butscher and Huggenberger, 2009).

There are many approaches to protect groundwater at a catchment scale; it either consist of treating water at the outlet before its supply into networks, or to a lesser extent prevent contamination at the source, i.e., ensure the protection of the recharge area of the water outlet (well or spring). In the latter case, there is a need to assess the distribution and type of recharge and infiltration occurring on the catchment, and highlight their vulnerability to contamination as a function of their contribution to the outlet.

The objective of this work is to understand infiltration on the complex Qachqouch karst catchment, to identify a hydrogeological connection between a Nahr el Kalb river and the highly polluted Qachqouch spring and to quantify potential infiltrations under various flow periods which will help highlighting the specific vulnerability of this spring to specific types of emerging micropollutants (MPs). For this purpose, tracer experiments were conducted on a surface water basin to determine this link to an adjacent groundwater recharge

area and a karst spring. Furthermore, the frequency of occurrence of selected persistent micropollutants (MP) was assessed on this surface water basin, once the connection and transport characteristics were established. This was done by monitoring the MPs in the spring and river under various flow conditions, in order to assess their impact on the groundwater karst system. Additionally, the monitoring of the spring following a multi precipitation event allowed characterizing the fast infiltrated component arriving at the spring and the breakthrough and loads of indicator MPs: Sucralose (SUC), Acesulfame-K (ACE-K), Gemfibrozil (GEM), Iohexol (IOX) and their various origins. As such, the efficiency of these selected MPs as wastewater indicators in karst systems was further evaluated.

Ultimately, this study aims to provide decision makers with a conceptual understanding of wastewater type, consumption loads, and point sources along the river and needs for treatment in rural settings.

Following this introduction, part 2 will present an overview of the background studies related to 1) karst aquifers, 2) vulnerability, 3) artificial tracer experiments, and 4) usage of MPs as indicators of specific vulnerability. Part 3 describes the field sites of the Qachqouch spring and Nahr el Kalb River. Part 4 presents a detailed methodology including field and laboratory methods, as well as the analytical methods used to evaluate the results. Part 5 contains results of the tracer tests, the occurrence of selected domestic and hospital emerging MPs on a rural surface water basin linked to a groundwater karst catchment, as well as the assessment of the origin and transport of four selected emerging MPs; SUC, ACE-K, GEM, and IOX in a karst spring during a multi-event spring response. Part 6 presents an elaborate discussion of the results. Finally, concluding remarks are provided in 7.

CHAPTER 2. BACKGROUND STUDIES

2.1 Introduction to karst systems

Karst features are formed by dissolution of rocks, such as carbonates. The dissolution of hard rock allows groundwater movement within them by forming underground drainage systems such as sinkholes, caves, conduits, and fissures. (Ford and Williams, 2007). They are recharged through rapid concentrated infiltration (autogenic), which can be significant in dolines and/or dry valleys, and/or holes, and/or sinking streams. They can also be recharged by diffuse (allogenic) infiltration through soil and epikarst, which is more or less homogenous over the entire catchment area, forming a relatively thick unsaturated zone (Goldscheider & Drew, 2007).

2.2 Karst heterogeneity

Generally, karst aquifers are heterogeneous; meaning they may have conduits where water flows easily or massive unproductive rock only a few meters apart. Heterogeneity also implies that hydraulic parameters, recharge, and flow are all difficult to predict (Baedke and Krothe, 2001; Butscher and Huggenberger, 2009; Goldscheider, 2002), because of the duality of porosity, storage, flow and infiltration.

There are three major types of karstic features; exokarstic, epikarstic, and endokarstic. Exokarstic is subaerial, epikarst is defined as the top of karstified rocks, where fissures are abundant, and endokarst are subterranean. Some examples of dissolution karstic features include karrens which are centimeters to meters concave landforms; and dolines, which are subcircular depressions that can reach sizes varying from meters to hundreds of

meters. Larger scale landforms include uvalas and poljes, which follow geological structures such as synclines and grabens (Goldscheider & Drew, 2007). These structures denote important groundwater point source infiltration (Figure 2-1).

Additionally, a duality of flow can be observed in the saturated zone of karst aquifers (Figure 2-1). A conduit system may range from a few cm enlarged fractures to large and enlarged dissolution caves, and interacts with matrix porosity storage. Therefore, hydraulic conductivities may often reach $>100\text{m/h}$, and may be turbulent, whereas matrix hydraulic conductivities are much lower (Goldscheider & Drew, 2007). Storage in conduits is also low, so the resulting conduit systems occur where a fast flow is draining low permeability matrix storage (Doummar et al., 2012, Geyer et al., 2007; Kiraly, 2002).

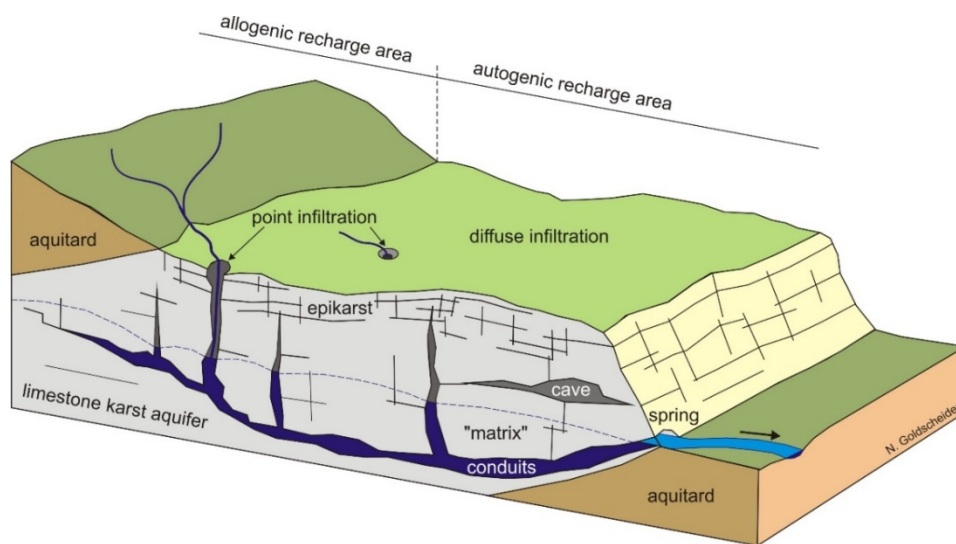


Figure 2-1. Schematic representation of a karst aquifer portraying the duality of flow and recharge (concentrated vs diffuse) in karst aquifers (after Goldscheider, 2007)

2.3 Specific and intrinsic vulnerability of karst systems

Karst aquifers are characterized by low transit times and fast flow pathways, which makes the potential contaminant migration high and rapid (Doummar et al., 2018, Field,

1990, Hamdan, 2018). So, mitigation of contamination is not likely to occur naturally (Vias et. al, 2006). They are characterized by rapid reaction to precipitation events, i.e., water level may rise rapidly and drastically (Goldscheider & Drew, 2007). The behavior of karst systems is studied by the combination chemographs, hydrograph, and discharge (Smart 1988; Williams 1983). Since the response of karst aquifers to storm events may be rapid, contaminants will be as quick to reach the aquifer as well. Therefore, the assessment of sensitivity of karst aquifers to contamination and protection of recharge zones that are at potential risk of contamination, are to be done in order to secure a sustainable management of water resources (Bakalowicz, 2005). This is done by predicting the contaminant arrival time, maximum concentration, and concentration time, in order to decrease contamination or allow sufficient time for remediation. This should take into account the contaminants, as well as aquifer properties (Figure 2-2). These parameters are crucial in studying the sensitivity, and vulnerability of karst catchments to contamination (Doummar et al., 2018).

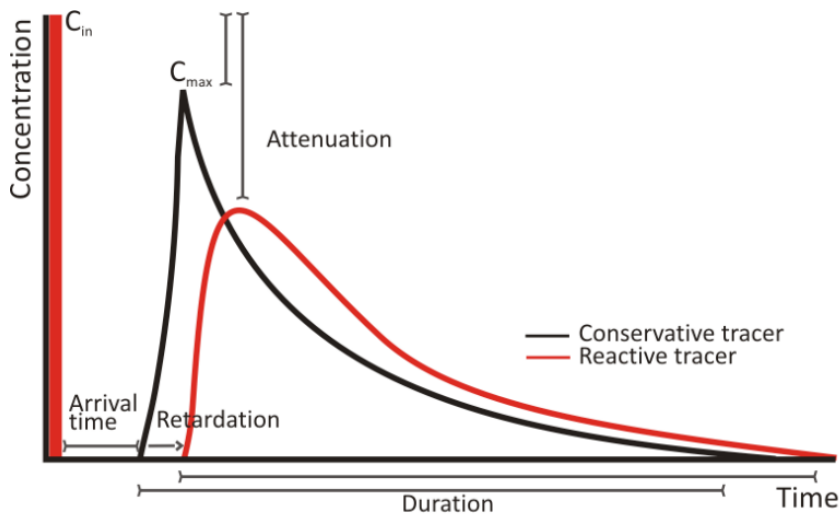


Figure 2-2. Figure showing concentration vs time of various possible responses of curves depending on geometry, transport parameters, flow (Modified from cost action 620, 2003 in Doummar, 2012)

Karst aquifer vulnerability is characterized by assessing flow and transport at a catchment scale using field investigations, subsurface characterization through surface experiments and data analyses. These include artificial tracer tests and spring responses such as hydrograph and chemograph analyses (Atkinsons, 1977). The objective of vulnerability of karst is to determine the recharge origin, type of infiltration, type of flow of the groundwater, and transit time.

Vulnerability is defined as the sensitivity of an aquifer to contamination exposure (Foster, 1987; Margat, 1968). Contaminants originate at a point source, are transported in a path through the unsaturated and saturated zones, and arrive to the outlet (spring or well; Neukum et. al, 2008; Figure 2.3).

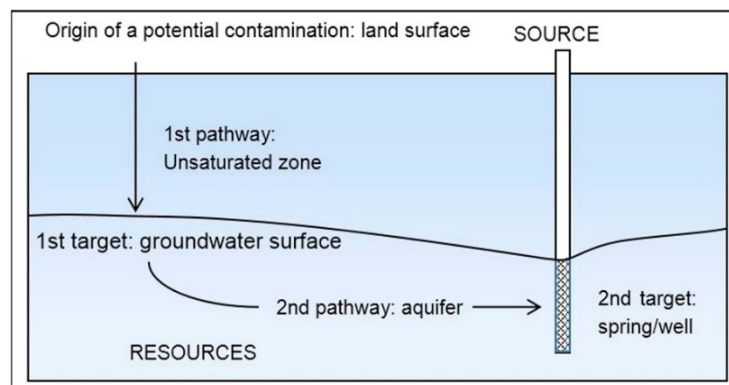


Figure 2-3. Origin-pathways-target concept of vulnerability assessment (Goldscheider, 2002)

There are two types of vulnerabilities; intrinsic and specific. Intrinsic vulnerability represents the media's sensitivity; for example geological or hydrogeological properties of an aquifer, independent to type of contaminant (Civita, 2010; Vias et. al 2006). Specific Vulnerability refers to the characteristics of the contaminant, such as MPs, or human activity; their transport parameters, biodegradation, sorption, and transit time. Methods to assess vulnerability include artificial tracer experiments, and calculation of velocities, dispersions,

mass etc... Potential pollution sources on the catchment should be located and identified in order to assess their impact on the karst aquifer. Moreover, the relationship between anthropogenic tracers, such as MPs, and spring response curves of turbidity, chloride, electrical conductivity and calcium can be used and correlated (Pronk et al., 2008).

2.3 **Methods of characterization in karst systems**

2.3.1 *Artificial tracers and experiments*

There are three types of artificial tracers; fluorescent dyes, salt tracers, and drifting particles. Fluorescent dyes are colored substances that dissolve in water or aqueous solutions. Salt tracers are inorganic compounds that dissociate in aqueous solutions into cations and anions. Drifting particles are particles that stimulate the behavior of contaminants and/or microbial pathogens. Artificial tracer tests are field experiments where a substance is introduced into the water system that can be tracked and identified at another site (Kaess, 1998).

2.3.1.1 Applications of tracer tests

Artificial tracers are applied in hydrogeology to identify a connection between a source and an outlet; knowing and tracing origin, and destination of water (Morales et. al, 2007; Smart, 1988). According to Kaas (1998), tracer injection sites in karst regions are chosen where water percolates continuously, on swallow-holes for example, or cave water systems such as Doummar et al. (2018), or on dolines with little soil cover to allow water to flow directly into the conduits (Kaess, 1998). In some cases, as with the case of this study, fluorescent tracer dyes are injected on surface water systems to establish a connection between surface water and groundwater networks. Number of conduits from source to outlet can also be determined from the amount of tracer breakthrough curves (single peak vs

multiple peaks.) Moreover, statistical and numerical analyses of the breakthrough curves allow estimation of parameters such as tracer recoveries, transit times, velocities, dispersion, and dispersivity. Observation sites are where water outlets exist; such as springs and/or wells, where monitoring equipment are installed. In addition, artificial tracer tests are used to delineate karst catchment boundaries, and to determine flow, transport, and attenuation/fate of matter in water and karst systems (Doummar et al., 2018; Morales et al., 2007; Smart, 1988).

2.3.1.2 Interpretation of tracer tests

The groundwater flow and transport with respect to hydrogeological significance is evaluated and interpreted using tracer tests (Fetter, 1999). Transport parameters of artificial tracer tests are governed by groundwater flow direction, dispersion and velocity (advection) (Figure 2-4).

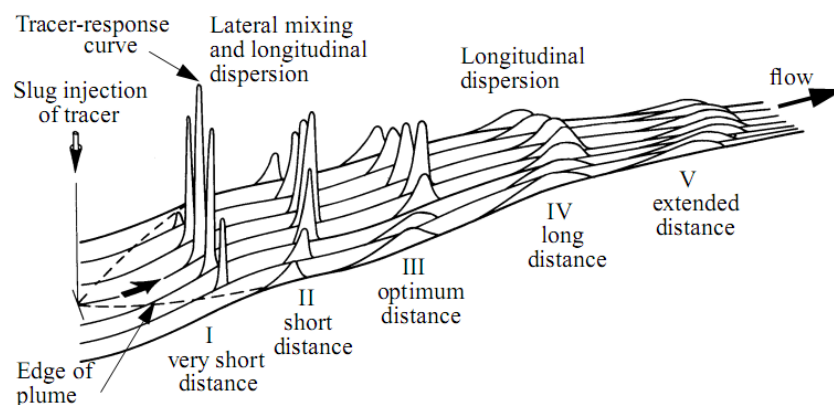


Figure 2-4. Extent of lateral mixing of the tracer and longitudinal dispersion over a distance following a Dirac injection pulse. Effect of dispersion on the variation of the peak concentration (Kilpatrick, 1993 in Doummar, 2012)

However, it is the mean velocity that is estimated, since a tracer cloud does not flow in water at the same velocity. Velocity in the middle of a fracture will be higher than

velocity at the sides of a fracture, owing to friction. This difference of velocity in a tracer injection will form a Gaussian curve when time is plotted against concentration of the tracer cloud. Velocity, or advection, is simply the flow velocity of the groundwater. The Gaussian curve can be flat and wide, or long and narrow depending on the velocity and concentration of the tracer; which in turn depend on the underground path of the aquifer. The latter is referred to as hydrodynamic dispersion (Figure 2-5)

Dispersion thus portrays the varying velocities of flow during transport; it controls the shape of the tracer breakthrough curve where, the distance of measurement from the source of tracer injection controls the breakthrough curve shape, which is determined from the concentration of the tracer reaching the outlet. Dispersion is the most important in flow direction in karst conduit's turbulent flow (Bear, 1979). Plotting concentration against time gives a Gaussian bell-shaped curve called a tracer breakthrough curve. The features of a breakthrough curve are the rising limb, the peak, and the recession. The curve can be symmetrical or asymmetrical. The asymmetry or a tailing breakthrough curve is caused by dispersion and storage (Figure 2-5). Retardation shifts the curve towards greater time of arrival values. In karst aquifers, the breakthrough curves reflect the structure of the flow path (Goldscheider & Drew, 2007).

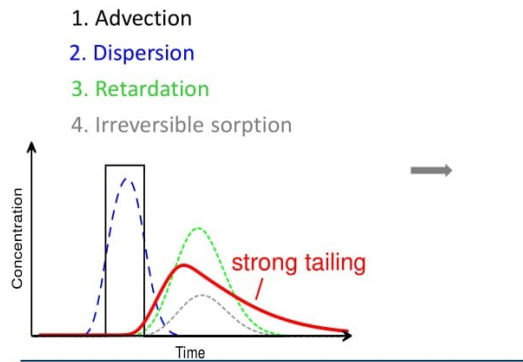


Figure 2-5. Breakthrough curves showing advection, dispersion, retardation, sorption, and tailing.

As mentioned earlier, a number of parameters can be calculated from tracer tests (Table 2-1). Travel time can be calculated if there is a measured distance between the injection point and the sampling/observation point. Calculation of travel time is important in vulnerability studies to determine whether there will be enough time for a contaminant to degrade or not during its transport. However, it is best to talk about travel time in terms of first detection limit (Goldscheider & Drew, 2007). Since the first arrival depends on the analytical detection limit of the equipment used to sample and log. Mean transit time can be computed statistically (Smart, 1988b). Mass recovery or the percentage of the injected tracer that was recovered at the sampling site can be calculated integrally. It is highly significant in order to determine a connection between injection and sampling point, to quantify that connection, to determine maximum concentration, and concentration time (Goldscheider & Drew, 2007). All of these variables are comparable with contaminants, which is important in vulnerability studies of an aquifer.

Parameter	Symbol	Description
Tracer Recovery	M_r	Mass Recovered
Mean Tracer Velocity	v_m	Velocity of flow
Mean Transit Time	t_m	Time for half the tracer to cross the aquifer distance
Maximum Velocity	v_{max}	Time of the first arrival of tracer cloud
Longitudinal Dispersion	D_L	Rate at which the tracer mass spreads out along a flow path
Longitudinal Dispersivity	α_L	Length of tracer cloud dispersion
Peclet Number	P_e	Reflective of the contribution of each of the mechanical dispersion and advection flow onto mass transport
Conduit/Channel Dimensions	Φ, A	Channel diameter, Cross sectional area/ surface area,
Portion of mobile Phase and exchange coefficient between immobile and mobile	β, ω	Required to define the behavior of the mobile fluid phase and the exchange between mobile and immobile phases

Table 2-1. Table showing parameters that can be calculated numerically and statistically from artificial tracer tests

The form of a breakthrough curve provides even more information on the underground conditions. A single peak suggests a single conduit. Multiple peaks may indicate multiple conduits. Some of the tracer may be directed into storage which can be on the conduit route, or off its route and does not allow exchange (Goldscheider & Drew, 2007). Sustained tails can result from storage as well when there is an exchange; but it may also result from unresolved multiple peaks (Werner et. al, 1997). Measurement of discharge is very important in tracer tests, and they provide greater resolution results when compared with injected and recovered mass. Also, tracer tests under varying flow conditions (varying discharge) may reveal changes in the underground conduit velocities, paths, and storage (Smart, 1988b). Figure 2-6 shows network configurations of karst networks. Where M is mass of tracer injected and Q is discharge. In A, $Q_{in} = Q_{out}$, therefore, $M_{in} = M_{out}$. In dilution convergence, B, $Q_{out} < Q_{in}$, so Mass recovery will be less than 100%. In divergence, as in

example C, $Q_{in} > Q_{out}$, therefore $M_{in} > M_{out}$. In the case of divergence convergence, as in D, and convergence divergence as in E, $Q_{in} \neq Q_{out}$, $M_{in} \geq M_{out}$. When there is no connection as in drawing F, $Q_{in} \neq Q_{out}$, M_{out} is equal to 0, no tracer detected. In the case of G, where exchange occurs with a storage through a conduit. In H, there is storage in line, and in I, there is a bypass system. In G, H, and I, $Q_{in} = Q_{out}$, and $M_{in} = M_{out}$, and the tracer breakthrough curve will show tailing.

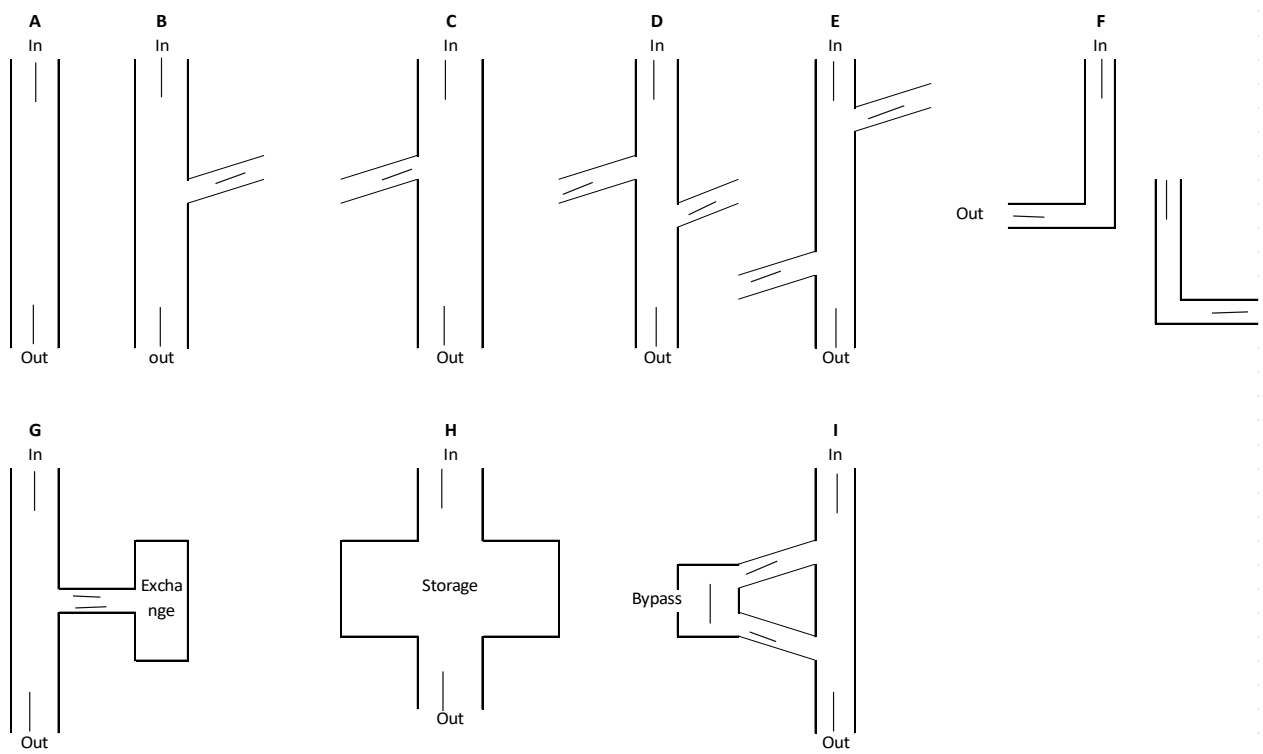


Figure 2-6. Karst network configuration based on measurement of input and output, discharge, and tracer recovery. (after Ashton 1966, Atkinson et al. 1973, Brown & Ford 1971, Brown and Wigley 1969, Smart 1988a.)

2.3.1.3 Analytical models of transport parameters

Karst aquifers are difficult to model due to their heterogeneities, anisotropy, and varying conduit scales. The modeling approach was to transform an input signal into an output signal with an analytical equation that substitutes for the physical properties of the

aquifer. A best-fit approach method is used in order to model the curve that fits the data series (Goldscheider & Drew, 2007). The type of model used depends on the shape of the curve, for instance, it is enough to use an Advection Dispersion Model (ADM), for a normal bell shaped curve. If a curve shows strong tailing, then a Two Region Non-Equilibrium Model (2RNEM) is used, since it allows the estimation of mean tracer velocity, longitudinal dispersion, the assessment of the portion of immobile region and the exchange between immobile and mobile regions (Doummar et al., 2018, Field and Pinsky, 2000; Geyer et al., 2007).

2.3.2 Natural tracers: stable isotopes

Natural tracers, stable isotopes, Deuterium (^2H) and Oxygen (^{18}O) are used to track origin of water and its movement. The abundance of ^{18}O to ^{16}O of these natural isotopes varies as they fractionate from temporal and/or spatial elements, which makes them conservative tracers (Criss, 1999). Fractionation is the separation of isotopes among the different phases and measures the abundance of the ratio of isotopes due to processes such as evaporation. For ^2H and ^{18}O , standard mean ocean water (SMOW) is used as reference material (O'Neil, 1986). ^2H and ^{18}O are considered heavy as it has lower vapor pressure than ^1H and ^{16}O , as a result, ^2H and ^{18}O concentrations are higher at higher elevations (Dansgaard, 1964). In simpler terms, generally, air masses will lose water content and hence the lighter isotopes as they move inland and to higher elevations from the coast where the heavier isotopes are retained. Stable isotopes can be used to determine altitudes of recharge/infiltration and or likelihood of mixing between water of different origin.

2.3.3 Spring chemograph and hydrograph analyses

A chemograph is based on physical and chemical measurements collected at the spring. Measurements include electrical conductivity (EC), temperature, pH, turbidity (TU), major ions, and stable isotopes (Sauter, 1997). Electrical conductivity increases with the number of charged ions in water, which shows an increase when stored water, rich in minerals, is measured and logged in the field. Major ions in chemographs are suitable to estimate origin and mixing proportions of new waters, stored groundwater (Ca and Mg), and wastewater (Cl). Turbidity can be a good indicator of fast pathways conduits from sinking streams outside the karst catchment into the spring; primary and secondary turbidity peaks result from autochthonous and allochthonous sources respectively (Pronk et. al 2006, Sauter, 1992).

In this study, relationships were established by combining different chemographs, hydrographs, discharge, (Williams, 1983), isotopes (Criss, 1999), and MPs. Moreover, discharge is important in order to quantify the mass flux, which is the product of concentration and discharge, in order to remove the effect of dilution (Smart, 1998). By combining discharge, EC, TU, ion concentration, and isotopes, we can tell if newly infiltrated water is mineralized, infiltrated through fast pathway, and is from a groundwater or contaminated with wastewater. Figure 2-7 shows an example of a karst spring monitoring where new (lower Mg compared to Ca) and highly mineralized (high EC) water arrived at the spring during a flood event (high discharge).

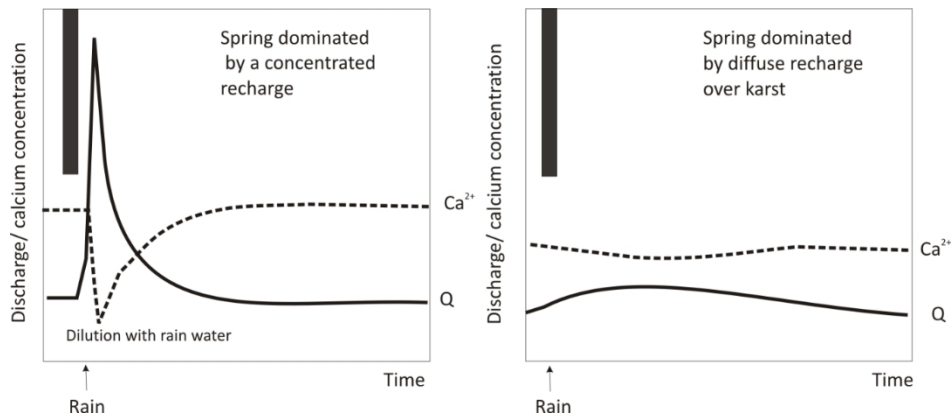


Figure 2-7. Combination of hydrographs and chemographs to understand karst aquifer behavior (Ford and Williams, 2007)

Relationships between discharge, transit time, dilution and concentration in vulnerability are also important to identify and are presented in figure 2-8.

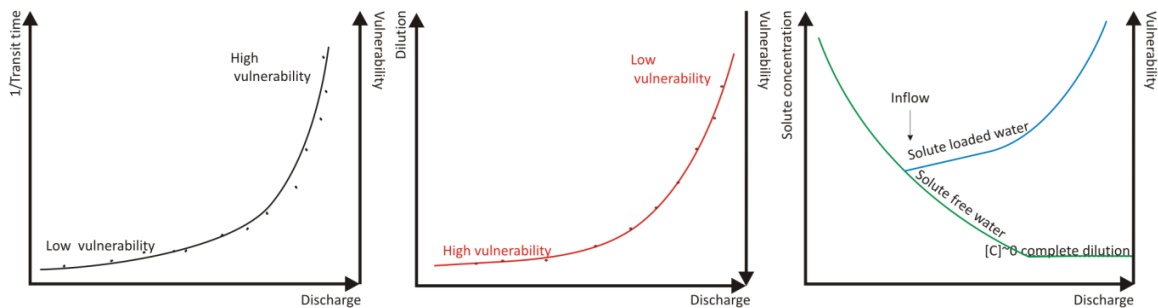


Figure 2-8. Relationship between discharge and transit time, dilution and solute concentration in a system and their relevance to vulnerability (from Doummar, 2012).

2.3.4 Micropollutants

Healthcare products such as preservatives, antimicrobials, and antibacterial; pharmaceuticals such as antibiotics, anti-inflammatory, hormones; contrast media; industrial manufacturing products; animal care (farming); agriculture products etc. All are increasingly used in modern industry, especially in urban areas. They are often released into wastewater treatment plants, directly into soil, or into surface water, and proceed to leach into groundwater. Their signature in water is in the form of MPs that can be detected to various extents in raw wastewater and treated wastewater, if persistent or in groundwater and surface

water. A wastewater indicator is defined as 1) having an exclusive origin from wastewater, 2) abundant in wastewater above detection limits, 3) found at low concentrations in the investigated system, 4) characterized by a low degradation rate and negligible retardation (Doummar et al., 2014, Gasser et al., 2010, Einsiedl et al., 2010).

The contamination of groundwater resources by MPs is a growing and relatively poorly understood concern. In the last few decades, the fate of MPs in the natural environment has been studied by assessing their degradation, and their transformation products. (Daughton and Ternes, 1999; Halling- Sørensen et al., 1998; Kümmerer, 2009; Lim, et al., 2017; Schwarzenbach et al., 2006; Stan and Linkerhagner, 1992; Stan et al., 1994). MPs are present in wastewater, treated wastewaters, surface waters, and groundwater (Reh et al., 2013; Scheytt et al., 2006.) However, they are not regularly monitored and analyzed due to high costs and absence of regulatory requirements.

Table 2-2. A list of micropollutant categories occurring frequently in the environment mostly in aqueous systems.

Categories	Subcategories	Compounds	Categories	Subcategories	Compounds		
Pharmaceuticals	Antibiotics	Amoxicillin (semi-quantitative)	Personal Care Products	Anti-Bacterial	Carbadox		
		Azithromycin			Sulfamerazine		
		Erythromycin			Sulfamethazine		
		Flumequine		Sulfathiazole			
		Trimethoprim		Triclocarban			
		Lincomycin		Triclosan			
		Oxolinic acid		Anti-Microbial	4-nonylphenol		
		Quinoline			4-tert-Octylphenol		
		Sulfadiazine			Butylparaben		
		Sulfadimethoxine		Sulfachloropyridazine			
	Sulfamethizole	Preservatives	Isobutylparaben				
	Sulfamethoxazole		Methylparaben				
	Anticonvulsant	Primidone	Propylparaben				
	Heart and Blood Treatment (β Blocker)	Atenolol	Agricultural/Industrial	Herbicides	Chlorotoluron		
		Bezafibrate			Diuron		
		Dehydronifedipine			Isoproturon		
	Lopressor	Metazachlor					
	Nifedipine	Metolachlor					
	Warfarin	OUST (Sulfameturon,methyl)					
	Steroids/Hormones	Androstenedione			Propazine		
Testosterone		Simazine					
Norethisterone		Thiabendazole					
Progesterone		2,4-D					
Analgetics, Anti-inflammatory, Anticonvulsants	Estradiol	Clofibric Acid					
	Estradiol	Salicylic Acid					
	Estrone	Pesticides	Atrazine				
	Ethinyl Estradiol - 17 alpha		Bromacil				
Lipid regulator	Acetaminophen	Food Additives	Artificial Sweeteners	Chloridazon			
	Albuterol			Cyanazine			
	Carbamazepine			DEET			
	Carisoprodol			Linuron			
	Cimetidine			Industrial	DACT		
	Diazepam				DEA		
	Dilantin				TCCP		
	Diltiazem				DIA		
	Contrast Media			Fluoxetine	Stimulants	Psychotropic	BPA
				Ketorolac			TCCP Flame retardant
Lidocaine		TDCPP					
Meclofenamic Acid		TCEP Reducing Agent					
Food Additives	Meproamate	Food Preservatives	Ethylparaben	Acesulfame-K			
	Pentoxifylline			Sucralose			
	Bendroflumethiazide	Theobromine					
	Butalbital	1,7-Dimethylxanthine					
Chloramphenicol	Caffeine						
Tobacco related	Gemfibrozil	Nervous	Theophylline				
	Iohexol						
	Iopromide			Cotinine			

Previous studies done by Buerge et al, 2009, Doummar et al., 2014, Gasser et al., 2010, Liu et al, 2014, Mawhinney et al, 2011, Nödler et al, 2016; Oppenheimer et al, 2011, Stempvoort et al, 2013; Wolf et al, 2012, investigated the use of some persistent MPs as wastewater indicators. Some studies relied on their concentrations in the environment to estimate the prescribed dosages or consumption loads (e.g., cocaine, and caffeine; Hillebrand et al., 2011, Zuccato et al., 2005), and to assess their transport characteristics in hydrological and hydrogeological systems. According to Oppenheimer et. Al (2011) the characteristics of an ideal wastewater indicator after treatment are 1) Source specificity, 2) Sustained effluent release, 3) Available high resolution analytical methodology, 4) limited attenuation during transport and treatment, 5) Nearly zero background concentration.

Various studies have outlined wastewater indicators in surface and groundwater for water quality monitoring purposes (Clara et al., 2004; Doummar et al., 2014; Gasser et al., 2010; Hillebrand et al., 2014). The dosage of selected pharmaceutical products and their release in the environment is presented in table 2-3. The fate of selected MPs has been investigated in details in terms of degradation, half-lives, and metabolite release in the environment. Nevertheless, there is an urgent need to investigate the occurrence and fate of other selected MPs under specific hydrological conditions (Lim et. al, 2017), before assessing their suitability as wastewater indicators in the environment, especially in challenging karst systems. Recent studies have documented the occurrence of artificial sweeteners (ASW) such as SUC, and ACE-K in the aquatic environment (Brorstroem-Lunden et al, 2008; Buerge et al, 2009; Loos et al, 2009; Mead et al, 2009; Scheurer et al, 2009), along with the lipid regulator gemfibrozil (Araujo et al, 2011; Bendz et al., 2005; Sanderson et al., 2003) and the contrast media iohexol (Kormos et. al, 2011, Putschew et. al, 2000).

Table 2-3. Selected micropollutants, consumption per person per day (kg/day when specified), half-lives in natural water, and metabolites

Micropollutant	Consumption (mg/day unless otherwise specified)	Half-Life (Hours)	Metabolites	Product of	References
1,7-Dimethylxanthine	-	1	-	Caffeine	Bortolotti et. al (1985); Guerreiro et. al (2008)
2,4 D	-	11.6	Sulfamic Acid	-	Sauerhoff et. al (1977)
Acesulfame-K	1.22	3240	Glucuronide and Sulfate	-	Subedi and Kannan (2014); Castronova et. al (2017); Inchem.com
Acetaminophen	4000	40–350	Penicilloic acid and phenol hydroxypyrazine, diketopiperazine, AMX-S-oxide	-	Andreozzi et. al (2003); Drugs.com
Amoxicillin (semi-quantitative)	1000	48-216	-	-	Andreozzi et. al (2004); Gozlan et. al (2013); Drugs.com
Atenolol	100-200	160	5. 1-[4-(C-Carbamoylhydroxymethyl)phenoxy]-3-isopropylaminopropan-2-ol	-	Liu and Williams (2007); Reeves et. al (1978); Dailymed.com
Bisphenol A (BPA)	-	24-240	-	-	Fox et. al (2007)
Caffeine	350	288	1,7-dimethylxanthine	-	Buerge et. al (2003);
Carbadox	<400	2.3	Quinoxaline-2-carboxylic acid	-	Keller et al (1981); Nabuurs et. al (1990)
Carbamazepine	1600 to 2400	2400–10,000	(di) & (epo) hydroxycarbamazepine	-	Andreozzi et. al (2003); drugs.com
Cimetidine	100s	50-150	-	-	Latch et. al (2003); Drugs.com
Cotinine	-	16	-	Nicotine	Booth and Boyland (1970); Jarvis et. al (1971)
Diclofenac	50-200	1.5	Hydroxy & Methoxy diclofenac	-	Galmier et. al (2005); Drugs.com
Dilantin (anti-seizure)	300-500	204	Hydroxyphenytoin, 5-(4'-hydroxyphenyl)-5-phenylhydantoin.	-	emedicine.medscape.com
Estradiol	1 to 5 /month	2	EE2	-	Stanczyk et. al (2013); Lin and Reinhard (2005);
Estriol	0.25	2.9	-	-	Heithecker et. al (1991); Lin and Reinhard (2005);
Gemfibrozil	1200	15	Acyl-GEM-glucuronide.	-	Ogilvie et. al (2006); Drugs.com
Ibuprofen	200-400	15	hydratropic acid, 4-ethylbenzaldehyde, 4-(1-carboxyethyl)benzoic acid, 1-(4-isobutylphenyl)-1-ethanol, 2-[4-(1-hydroxy-2-methylpropyl)phenyl]propanoic acid, 1-isobutyl-4-vinylbenzene, 4-isobutylphenol. For 1-(4-isobutylphenyl)-1-ethanol.	-	Lin and Reinhard (2005); Climent et. al (2012); Caviglioli et. al (2002); drugs.com
Iohexol	1-350 mg/kg	2	-	-	Greskowiak et. al (2015); Halme et. al (1993); drugbank.ca; medscape.com
Iopromide	3--60	1.65	-	-	Greskowiak et. al (2015); Ting et. al (2010); drugs.com
Ketoprofen	200	4.1	-	-	Lin and Reinhard (2005); drugs.com;
Meprobamate	1200-1600	10	Hydroxymeprobamate	Carisoprodol	Walkenstein et. al (1958); drugbank.ca
Meclofenamic Acid	50 to 400	0.9	-	-	Snow et. al (1981);
Naproxen	1000	1.4	-	-	Lin and Reinhard (2005); drugs.com
Nonylphenol	-	up to 99 days	-	-	Mao et. al (2012); Canada. National Guidelines and Standards Office (2002)
Quinoline	-	336-2952	Acyl and Phenolic Glucoronide	-	Kochany and Maguire (1994); Novak and Brodie (1950)
Salicylic Acid	0.1-0.3 (L/kg)	3	Aspirin Active Metabolite	-	Schröder and Campbell (1972); Kuehl et. al (2006); toxnet.nlm.nih.gov
Sucralose	5 (mg/kg)	several years	-	-	Grice and Goldsmith (2000);
TCEP	-	17520	-	-	Saint Hilaire et. al (2013)
Theobromine	-	7 to 12	8-hydroxylation to 1,3, dimethyluric acid, 1-methylxanthine3-methylxanthine	Caffeine	Mumford et. al (1996);
Theophylline	16-10 9mg/kg)	8.7	Protein adducts.	Caffeine	Schebb et. al (2012); Ying et. al (2007)
Triclocarban	-	2592 - 485	-	-	

ASWs are ubiquitous in the human diet, (Oppenheimer et. al, 2012) and are not extensively metabolized by humans (Roberts et. al, 2000). They are excreted unchanged in urine, flow into wastewater treatment plants or untreated wastewater, and are discharged directly to environmental waters. (Grice and Goldsmith, 2000; Hoque et al, 2014; Labare et al, 1993; Roberts et al, 2000; Sang et al, 2014; Sims et al., 2000; Wood et al., 2000).

Sucralose, sold under the trade name Splenda®, is a chlorinated form of Sucrose. It is approved for use as an additive in over 4000 food products in over 80 countries (Torres et. al, 2011). Acesulfame-K is also a calorie free sweetener, sold under the different commercial names, currently approved for use in the U.S.A (FDA, 2006). Due to their documented occurrence and persistence in surface water (Brorström-Lundén et al, 2008; Mead et al, 2009; Perkola et al, 2014) and groundwater; SUC, (Mawhinney et al, 2011; Oppenheimer et al, 2011), and ACE-K (Robertson et al, 2013), have been investigated as index tracers of domestic wastewater pollution in groundwater, (Buerge et al, 2009; Oppenheimer et al, 2011; Stempvoort et al, 2011; Stempvoort et al, 2013; Wolf et al, 2012) and surface water (Liu et al, 2014; Nödler et al, 2016; Spoelstra et al, 2013; Tran et al, 2014).

GEM is used as lipid regulator under various commercial names, and has a high persistence in the natural environment (Araujo et. al, 2009). Two percent (2%) or less of the consumed GEM is excreted unchanged (drugs.com/gemfibrozil), whereas IOX is a water soluble, low chemotoxic, and low osmolality contrast agent used for medical imaging (drugbank.ca). IOX is released into urine largely unchanged after passing through the body (drugbank.ca). Both IOX and GEM are not degraded by conventional wastewater treatment processes (Putschew et. al, 2001; Ternes and Hirsch, 2000); therefore they are also both considered markers for domestic wastewater or potentially, hospital waste in the case of IOX.

Ibuprofen is a nonsteroidal anti-inflammatory drug (NSAID) which works by reducing hormones that cause inflammation and pain in the body, (drugs.com, 2017). Nonylphenols (NON) are surfactants used in manufacture detergents and emulsifiers (Soares et. al, 2008).

CHAPTER 3. FIELD SITE

3.1 Nahr El Kalb River

The Nahr el Kalb River originates from Nabaa El Assal and Nabaa El Laban springs in the highlands of Kesrouane (Faraya-Sannine), in addition to interflow and runoff occurring shortly after rain events. Its catchment extends from the outlet of the River on the coast to about 22 km to the east in the Lebanese Mountains. Its southern and northern boundaries were delineated on topography highs. The river consists of three sub-catchments (RI -Nahr El Salib; RII-Nahr el Ouadi, and RIII- Nahr Abou Mizane) joining together to form the main branch of the River (Figure 3-1). Its yearly discharge reaches a maximum of 22 m³/s, whereas it runs dry during low flow periods, (from July-September of the hydrogeological year) with a total discharge yearly volume of 80-230 Mm³.

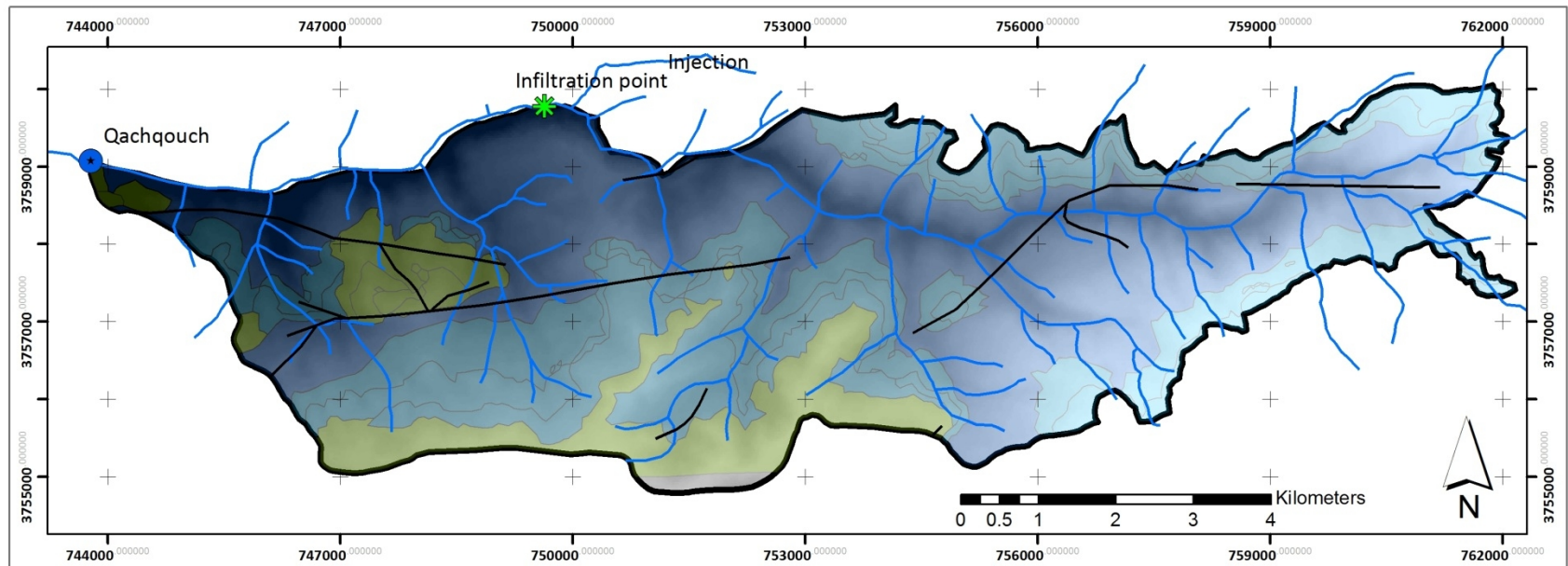
3.2 Qachqouch Spring

Qachqouch Spring (Figure 3-1) is located in the Keserouane area in Lebanon within the catchment of Nahr El Kalb; at about 64 meters above sea level, 18 km north of Beirut, draining a catchment that has been delineated and modeled to be about 56 km² (Dubois, 2017; Figure 3-2). Koeniger and Margane, (2014) outlined the elevation effect of ¹⁸O and ²H fractionation in the studied area, to determine spring water recharge origin for Jeita and Qachqouch. In their study, the values ¹⁸O and ²H from springs and from snow and rainfall were compared. The results showed that for both, Qachqouch spring and neighboring Jeita spring, the mean catchment elevation is higher than 1400 m asl, although the Jurassic Keserouane outcrop has a mean elevation of 1016 m asl. So, the higher elevation aquifers of

the catchment contribute a large percentage (as much as a 30% assumption) of recharge into both springs.

Qachqouch spring flows mainly in the Jurassic Keserouane formation (J4); it emerges at the contact between Bhannes formation (J5) and Bekfaya formation (J6), and passes through partially eroded Salima formation (J7) at 90 m above sea level. The direct recharge area of the Qachqouch spring consists of Kesrouane, Bhaness, and Bekfaya formation of Jurassic age. The Cretaceous formations of the highlands of Nahr El Kalb River (Chouf Sandstones (C1), Abeih formation (C2a), Mdeirij formation (C2b), Hammana formation (C3), and Sannine formation (C4)) are thought to contribute via overland flow (Figure 3-1). The Jurassic stratigraphy of Lebanon is summarized in figure 3-3.

The Jurassic formation is the dominant formation in the study area; and it is mainly formed of limestone, with intertonguing dolostones in the lower parts of the formation because of diagenetic dolomitization (Nader et al., 2007). The Jurassic massive limestones are often marked by karstification, but there are no known large water infiltration zones (Hahne, 2011).



Legend

- | | |
|------------------------------------|--|
| Points | Jurassic (Limestone-Dolostone J4) |
| Infiltration point | Upper Jurassic (Volcanics-Limestone J5-J7) |
| Qachqouch Spring | Cretaceous Strata (Sandstone- Limestone-Marly Limestone C1-C4) |
| Digital Elevation Model (m) | Faults |
| Value | El Kalb River |
| High : 1620 | Preliminary groundwater catchment |
| Low : 40 | |

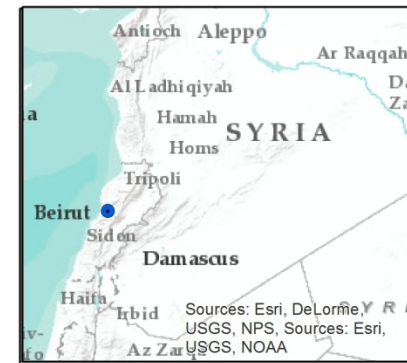


Figure 3-2. Overview map of the field site showing the catchment and geology of the Qachqouch Spring.

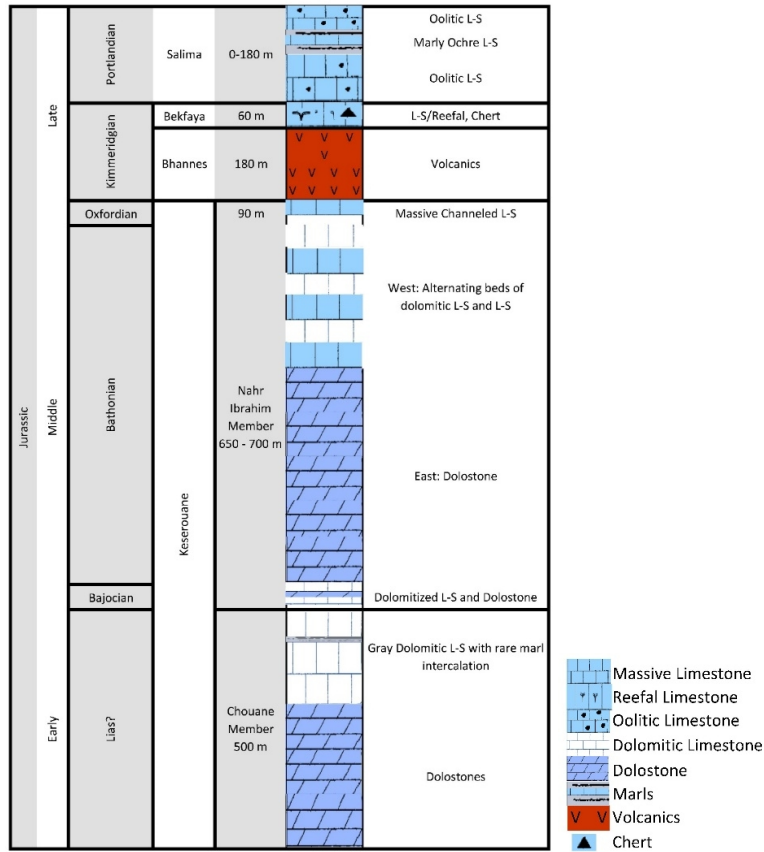


Figure 3-3. Jurassic stratigraphy of Lebanon (modified from Nader, et. Al 2007)

During low flow periods, the spring is used during water deficit in Beirut and surrounding areas. The total yearly discharge of Qachqouch Spring reaches 60 Mm³ based on high resolution monitoring of the spring (2014-2018). The discharge maxima recorded at Qachqouch Spring reaches 10m³/s for a short period of time following flood events. It's about 2m³/s during high flow periods and 0.2m³/s during recession (Figure 3-4). The total yearly precipitation is estimated to be 1000 mm on average, from one station deployed over the Qachqouch catchment at 950 m asl (2014-2018 local high resolution monitoring).

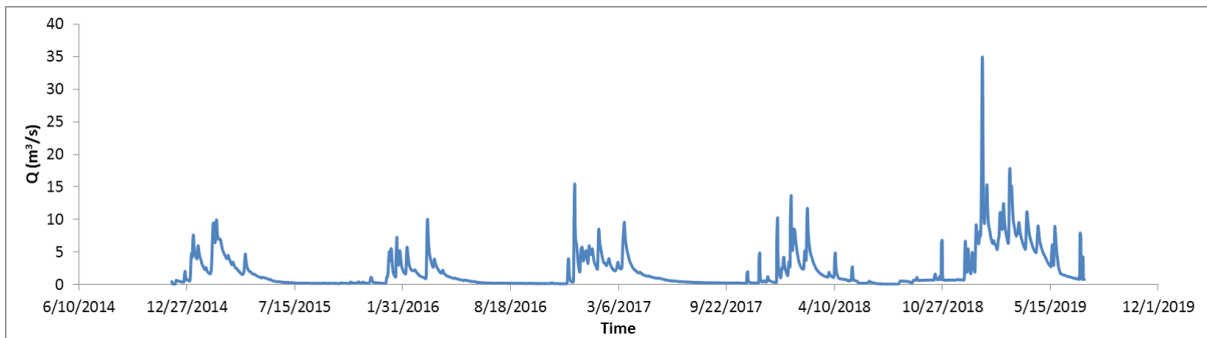


Figure 3-4. Qachqouch Spring Hydrograph showing discharge rates observed from 2014 to 2018 in 30 minute intervals using water level and recorded with a data logger (modified from Dubois, 2017)

Qachqouch Spring is about 100 meters downside of the Jeita Spring. 24 tracer tests conducted on the Jeita Spring revealed that there is no connection between it and Qachqouch Spring, proving that each of the two springs are independent (Doummar et. al, 2010a; 2010b; and Doummar, 2012). High resolution analyses of hydrographs and climactic data done by Dubois (2017) show that the Qachqouch karstic system has both transmissive and capacitive functions.

The system has been conceptualized by three different reservoirs emptying into each other to model the recessions and depletions. The model shows a quick response function which makes the spring reactive to rain events; and that is linked to fractured conduits that allow fast flow. A relatively slower reservoir, which is activated during the rainy season in between events, is probably linked to crushed limestone associated with dolomite (Nicod, 1971). A third and large storage reservoir, which along with the epikarst, gives the spring a storage-like behavior and keeps it flowing in depletion state during summer/dry seasons.

3.3 Surface and groundwater pollution sources

Qachqouch Spring is highly polluted due to excessive waste discharge located on its urbanized catchment upstream. Raw wastewater is either directly discharged into the river system or stored onto the catchment in bottomless septic pits or abandoned boreholes, since there are no effective wastewater treatment plants on the catchment area. During Lebanon's solid waste crisis (2015-2016), tons of unsorted waste was disposed in valleys along the catchments of both; the Kalb River, and Qachqouch Spring. Other sources of pollution include a poultry farm, solid waste dumps, hospitals, and quarries. The effect of these pollution sites can be detected in water samples as micropollutants.

CHAPTER 4. METHODS

4.1 Field methods

4.1.1 Spring monitoring

A multi parameter probe, In-situ 9500 XP, mounted with a chloride sensitive electrode was installed on the spring outlet. It continuously monitors and records electrical conductivity (EC), chloride (Cl), turbidity (Tu), temperature, pH, and water level in 20 minute intervals on a mounted data logger. The data is collected on site on field visits and analyzed using the software In-situ version 4, (Figure 4-1). Monitoring the spring during storm events was done in order to analyze fast flow water infiltration into the spring. During baseline, the spring was also monitored along with the identification of pollution sources on the catchment to assess specific vulnerability of the aquifer.



Figure 4-1. Left, Qachqouch Spring. Right, Probe installed at the Qachqouch Spring.

4.1.2 Physico-chemical and bacteriological sampling

Samples of water were collected from the Nahr el Kalb river (Figure 4-2), Qachqouch Spring and from rain during the storm event (600m and 900m asl) for major ions analyses: calcium, magnesium, potassium, sodium, bicarbonate, chloride, nitrate, sulfate, and nitrite. They were collected in plastic bottles, and were filled completely to inhibit exposure to the gas phase. They were refrigerated before being sent to the laboratory less than 24 hours after collection. Samples for bacterial analyses (*fecal coliforms*, *streptococci*, and *pseudomonas aeruginosa*), were collected in sterilized bottles.

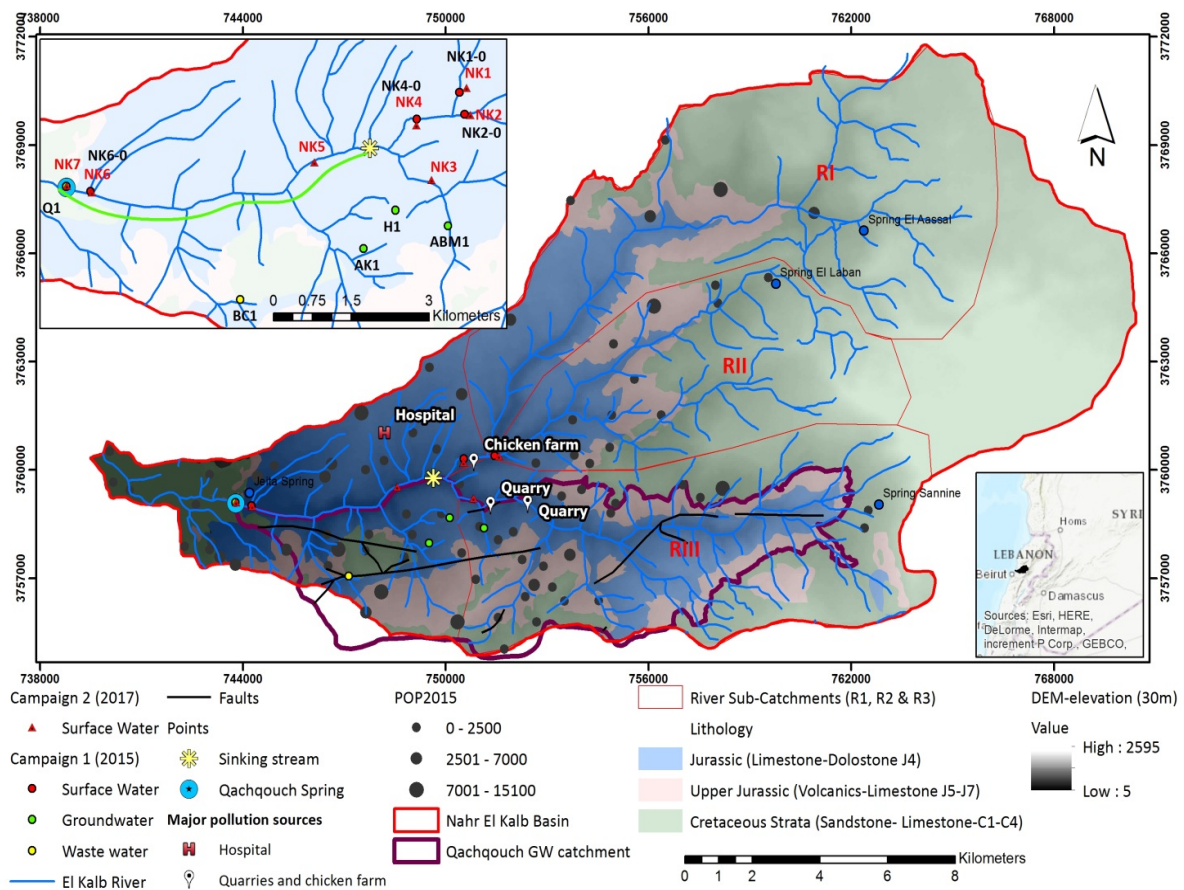


Figure 4-2. Geologic map of the field site: Nahr El Kalb River and Sampling locations during the two campaigns (POP2015 refers to number of inhabitants in 2015).

4.1.3 Micropollutant sample collection

Nine grab samples were collected in the first campaign in May 2015 following snow melt from various water outlets: (1) the Qachqouch Spring; (2) untreated municipal wastewater effluents facility; (3) three wells used for drinking and domestic purposes, and (4) four locations on the El Kalb River (including NK1-0, NK2-0 and two locations along the river; NK4-0 and NK6-0), where one of the samples lies directly downstream to a chicken farm (NK4-0). In the first campaign, sub-catchment RIII was dry.

In the second campaign undertaken in 2017, seven grab samples were collected for MP analyses, during the beginning of the snow melt period, from highly diluted surface water along the Nahr el Kalb River (Figure 3-1). The samples were collected from sub-catchments RI, RII, and RIII, as well as from four locations along the river (NK4–NK7). Between sample NK6 and NK7, about 300 L/s of overflowing groundwater are discharged into surface water, thus altering the water composition.

Three additional samples for the Qachqouch spring were collected in January 2016 during high flow (spring discharge varied between 0.3 and 7.5 m³/s during precipitation events).

The samples for MP analysis were collected in 40 mL amber glass vials and preserved in the field in a cooler with a 3 mg sodium omadine and 5 mg ascorbic acid. They were then transported on ice and preserved at temperature < 6 °C until sent to Eaton Eurofins Laboratories in California in coolers, a week after collection, to be analyzed. The analyses date is 2 weeks after collection. Both preservatives have been shown to be effective for stabilizing many pharmaceuticals and personal care products (PPCPs) for 28 days or more under these conditions (Oppenheimer et al. 2011).

All sample containers were provided by the laboratory and sampling was performed with chain-of-custody documentation (Oppenheimer et al. 2011). Samples of wastewater, surface water and groundwater were analyzed for 98 MPs for the first campaign.

4.1.4 Artificial tracer experiments

In order to assess the vulnerability of the karst aquifer by identifying mode of recharge, artificial tracer experiments were conducted. Moreover, to determine whether there is a connection between Qachqouch Spring and Nahr el Kalb sinking stream (Qachqouch Spring recharge through the river), to quantify the exchange, and to estimate transport parameters. Uranine (sodium fluorescein, BASF, CAS 518-47-8, $C_{20}H_{10}O_5Na_2$), was used as it is considered nontoxic to humans, animals and the environment, and it is conservative (Kaas, 1998). It has low detection limits (0.02 ng/l, under ideal conditions), it is considered highly soluble and it is visible in low concentrations (Figure 4-3), it is green above 10 ng/l and orange above 1g/l.



Figure 4-3. Tracer test preparation. Tracer cloud in Nahr El Kalb River

Three artificial tracer tests were conducted on 19/Feb/2016 (February Dye), 8/May/2016 (May Dye), and 24/Nov/2017 (November Dye). The injection was instantaneous and the point of the tracer tests was 8920 m from the Qachqouch Spring for May Dye and November Dye, a few hundred meters before the sinking stream (Figure 4-2, figure 4-3). Whereas February Dye was injected at Deir Chamra tributary of the river, 8700 m from the spring. Injection time was noted. Tracer concentrations were simultaneously monitored in the spring using a field fluorometer, GGUN-FL30 (Schneegg, 2002) that was calibrated for the applied tracers. The fluorometer measures and stores dye concentrations at the monitoring site at specific time intervals (every 15 min; Figure 4-4). During February 2016, another fluorometer was also installed downstream in the River close to the spring, in order to record the breakthrough curve at the river. When the concentration of tracer exceeded the maximum detectable concentrations, especially at the breakthrough peaks, samples were collected manually and stored away from day light, to be diluted up to 50 times and analysed in a lab at a later stage.



Figure 4-4. Field Fluorometer and data logger.

4.1.5 Discharge measurement

During the first campaign, discharge at the points of sampling was measured using the dilution method by injecting a non-toxic conservative artificial tracer (uranine sodium

fluorescein; CAS-518-47-8, C₂₀H₁₀O₅Na₂) with a known injection point, and measuring concentration with a field fluorometer mounted with a data logger (GGUN-FL30; Schnegg, 2002), ± 100 m downstream, depending on accessibility.

During the second campaign, the discharge of the river at the points of sampling was measured twice using an EM flowmeter (spacing interval between measurements of 10 cm); Valeport Model 801 (flat) (Figure 4-5). The calculated error of discharge measurement is 8%. Discharge at the spring is estimated with a calibrated rating curve and continuous water level monitoring.



Figure 4-5. Discharge measurement using EM Flowmeter

4.2 Laboratory methods

4.2.1 *Physico-chemical and bacterial analyses*

The 20 samples were further analyzed in the laboratories of Eaton Eurofins in California in the laboratory according to the method detailed in Oppenheimer et al. (2011). Analyses consists of a standard operating procedure using an online SPE coupled with a high performance liquid chromatographic separation with tandem mass spectrometric detection (SPE-HPLC-MS/MS). For extraction, Oasis HLB cartridges (2.1×10mm 25 μ) were used and

conditioned with 5 mL acetonitrile and 5 mL HPLC grade water acidified to pH 3 (Oppenheimer et al., 2011). Solid Phase Extraction column (SPE) allows complete extraction with good recoveries from aqueous matrices. The investigated MPs were analyzed in Electrospray Ionization (ESI) negative mode where an XBridge-C18 (2.1×150mm 3.5 μm particle size) column (Waters, Milliford, MA) was used for this purpose (Oppenheimer et al., 2011). The seven replicate of daily Minimum Reporting Limits Check – MRL_CHK, were based on 2.5 mL of spiked solution by using an online enrichment and back flush column switching method. The main analyzed MPs include wastewater indicators such as ASWs, lipid regulators, stimulants, analgesics, antibiotics, and anticonvulsants and anti-inflammatory drugs. In this work the two ASWs; SUC, ACE-K, GEM and IOX are of major interest for interpretation. The method quantification limit for SUC, ACE-K, GEM, and IOX were 100 ng/l, 20 ng/l, 5 ng/l, and 10 ng/l respectively, while the relative standard deviation for the compounds is 8.1%, 3%, 3.9%, and 4.5% respectively.

Ca was determined by means of ion chromatography (IC). A Dionex LC 20 with suppressor and conductometric detection, a Dionex CS12A column and a 20mM methanesulfonic acid eluent at a flow rate of 0.45 mL/min were used for the cations analysis. Additionally, prior to the analysis, 125 μl methanesulfonic acid 99% were added to each of the samples and stirred in a shaker for 2 hours. The Cl sensitive electrode was calibrated using three point calibration solutions in the field with a limit of detection of 1 mg/l).

Stable isotopes were analyzed using the high Temperature Conversion Elemental Analyzer (TC/EA) method for water analysis, with a standard deviation of 0.2‰ for ²H and ¹⁸O.

4.2.2 Micropollutant analyses

MP samples were analyzed in the laboratories of Eaton Eurofins in California, U.S.A by a standard operating procedure using an online SPE coupled with a high performance liquid chromatographic separation with tandem mass spectrometric detection (LC-MS/MS) as described by Oppenheimer et al., (2011). The seven replicate of daily Minimum Reporting Limits Check – MRL_CHK, based on 2.5 mL of spiked solution by using an online enrichment and back flush column switching method. Baseline and event samples were analyzed for both ES negative and positive. High flow surface water samples from snowmelt period were analyzed for mostly ES negative, only two locations were analyzed for ES negative and ES positive.

4.3 Analytical methods

4.3.1 Modeling of tracer breakthrough curves

The observed tracer breakthrough curves were analyzed numerically using the process-based model CXTFIT 2.1 (Toride et al., 1999). Tracer breakthrough curves were modeled using Advection Dispersion Model (Field and Pinsky, 2000; Geyer et al., 2007; Goepfert and Goldscheider, 2008). Reactive transport, i.e., decay and retardation will be discarded for the purpose of this work, as conservative tracers were used at a time. The physical parameters of the breakthrough curves (advection and dispersion in the case of ADM) were varied using the software until the modeled curves best fit the measured data. The modeled curve can then be applied to predict aquifer response. In karst aquifers, modeling the system is only a generalized model and does not represent the reality because karst aquifers are much more complex than the model (Goldscheider & Drew, 2007).

Advection and dispersion are both described by a 1- D partial differential equation, advection dispersion model, also known as ADM:

$$R \frac{\partial C}{\partial t} = D_L \frac{\partial^2 C}{\partial x^2} - v_m \frac{dC}{dx} - \mu C \quad \text{Equation 1}$$

x is the spatial coordinate [L], t is time [T], C is concentration [M/L³]. D_L is longitudinal dispersivity [L²/T], and v_m is effective mean velocity [L/T], μ is the decay constant [1/T]. In this study, geochemical processes are disregarded such as retardation and decay.

4.3.2 Discharge

Discharge [L³/T] is calculated integrally using the dilution method by the following equation:

$$Q = \frac{M}{\int_0^{\infty} C(t) dt} \quad \text{Equation 2}$$

Where M is mass of injected tracer, $C(t)$ is tracer concentration at time t , which is the area under the breakthrough curve.

When using an electromagnetic flowmeter, differential velocity is measured in incremental areas in the River (Figure 4-6). The discharge is calculated according to the following with an error of discharge measurement of 8 %.

$$Q = \sum_0^n v_i w_i d_i \quad \text{Equation 3}$$

Where v_i is the velocity [L/T] measured in the middle of each incremental area A_i [L²], w_i is the width [L] and d_i is the depth [L] of each incremental area A_i .

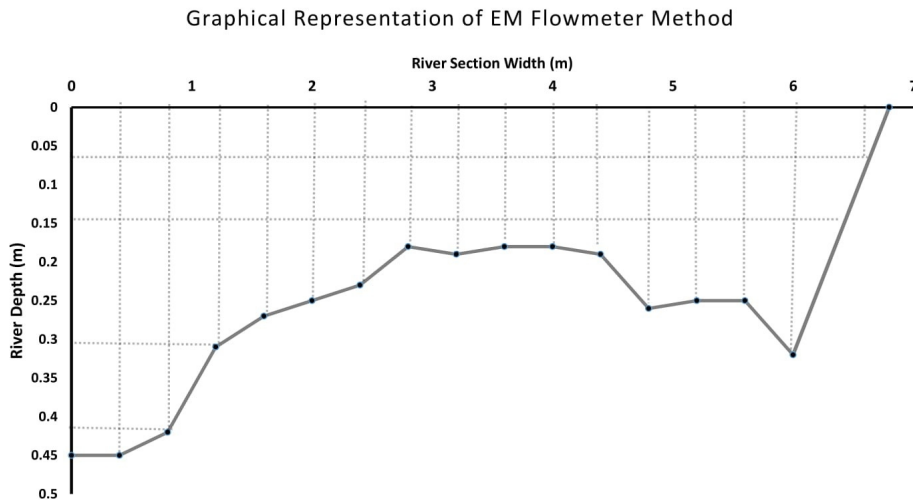


Figure 4-6. Graphical representation of EM flowmeter method on a Nahr el Kaleb River section

Moreover, at the spring, when discharge was not measured, it was estimated using the rating curve especially during storm events (Figure 4-7). The relationship can be determined graphically by plotting water level on the x axis, and discharge on the y axis, and getting the best fit of curve from the scatter of the data. Principally, this rating curve is established by making observations of the spring at different times under different flow conditions. Algebraically, discharge is calculated where water level is used as X in the polynomial equation of the curve, and a, b, and c are determined from the curve itself.

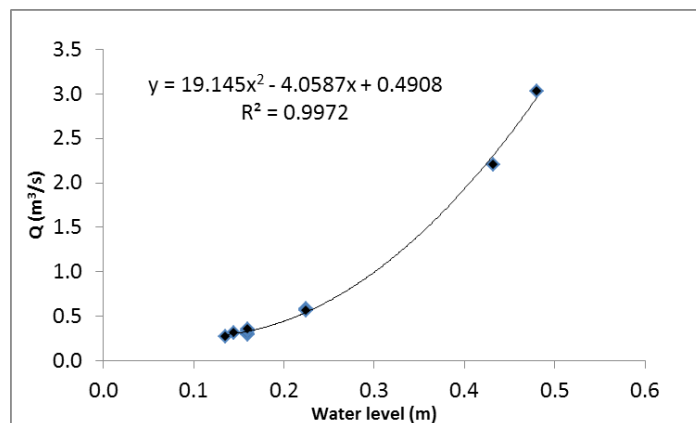


Figure 4-7. Polynomial rating curve showing the relationship between discharge and water level.

4.3.3 Origin of inflowing water

A mixing model based on calcium and bicarbonate concentrations was used to determine the origin of the inflowing water. The concentration of both ions in the additional flow into the river allowed the identification of its origin: i.e., interflow/surface water, groundwater or wastewater. In the case where the mass flux of chloride increases; a simple mixing model based on chloride, a conservative and typical for wastewater effluents (Gasser et al., 2010) was used to quantify the amount of wastewater change along the river system when the inflow is coming from inflowing river water.

$$\begin{aligned}
 M_w + M_{r(i)} + M_i &= M_{r(i+1)} \\
 C_w(XQ_i) + C_n(1-X)Q_n &= M_{r(i+1)} - M_{r(i)} \\
 Q_n &= Q_i + Q_w \wedge Q_i = \dot{V} \\
 X &= \frac{(M_{r(i+1)} - M_{r(i)}) - Q_n C_n}{Q_n(C_w - C_n)} \quad \text{Equation 4}
 \end{aligned}$$

Where M [M/T] is considered a mass flux and is equal to the product of concentration and discharge ($C*Q$). M_w is the mass flux of an ion in wastewater and M_i is the mass flux of an ion in inflowing water between $r_{(i)}$ and $r_{(i+1)}$, and $M_{r(i)}$ and $M_{r(i+1)}$ are the mass of the ion at two consecutive locations on a river at point i and i+1. X is the fraction of wastewater in the new inflowing water (Q_i ; [L³/T]) with a concentration of C_w (ion concentration in wastewater; [M/L³]). (1-X) is the fraction of inflowing water with concentration (C_n) of pristine river water. For Chloride, C_n is equivalent to 5 mg/l, while C_w is about 120-150 mg/l in the study area. When $M_{r(i)}$ is greater than $M_{r(i+1)}$, then the $X \geq 1$, the volume of wastewater added per unit of time is considered negligible, because of the effect of dilution.

4.3.4 Quantification of volume of new waters

The volume of new waters and percent of total discharge was estimated using a two- end mixing model (Equation 5) based on both Cl and Ca concentrations. It should be noted that the use of Ca underestimates the amount of new waters because of the water-rock interaction, especially in three consecutive events. The mass of Cl originating from wastewater in each event is considered negligible given the significant dilution.

$$\int C_n Q_n dt + \int C_b Q_b dt = \int C_m Q_m dt \quad \text{Equation 5}$$

With $Q_m = Q_n + Q_b$

Where C is concentration of Cl in rainwater (C_n), in mixed spring water (C_m) and pre-event spring water (C_b), Q_n is newly infiltrated waters, Q_b is baseflow, and Q_m is the mixed spring discharge water.

Based on Q_n and Q_b calculated above, the total mass of SUC and ACE-K referred to as MMP was estimated using a three end mixing model as follows (Equation 6):

$$M_{MP} + \int C_n Q_n dt + \int C_b Q_b dt = \int C_m Q_m dt$$

$$C_{MPm} V_m = C_{MPn} V_n + C_{MPb} V_b + M_{MP}$$

$$M_{MP} = C_{MPm} V_m - C_{MPb} (V_m - V_n) \quad \text{Equation 6}$$

Where (C_{MP}) is the concentration of the artificial sweetener (ACE-K and SUC) in the volume of mixed spring water (V_m), Volume of precipitated newly infiltrated water (V_n), and pre-event waters (V_b). M_{MP} is the new mass of artificial sweetener introduced to the spring. The concentration of MP in precipitation water is considered nil.

4.3.5 Estimation of recharge altitude based on isotopic signature

Estimation of the recharge elevation of event waters was estimated based on a comparison of spring signature during and post precipitation events to the meteoric precipitation isotope line (Koeniger and Margane, 2014).

4.3.6 Standard deviations and regression analysis

Statistical methods were used to measure the extent of correlation between parameters measured at the spring; such as concentrations, mass fluxes, and turbidity. They were defined based on the coefficient of determination R², by plotting the data (concentrations and mass fluxes of MPs and minerals) and observing whether there is a linear association of the two plotted variables. A good correlation means they have a similar origin, and it is implied when R² is between 0.65-1).

Moreover, a mean transit time (t_m; the time between the start of the rain event and the time where 50% of the mass flux had elapsed at the spring) was calculated for each of the four MPs and turbidity in events 1 and 2. The variance of the signals mass fluxes with respect to a mean transit time was estimated using Equation 7. A low variance is indicative of a higher skewness of the breakthrough curve while a higher variance would imply a longer duration of the compound's breakthrough.

$$\sigma^2 = \frac{(t_i - t_m)^2 \int C_i(t) Q_i(t)}{\int C(t) Q(t) dt} \quad \text{Equation 7}$$

Where σ^2 is the variance [T²] of the mass flux breakthrough curve with respect to a mean transit time (t_m: [T]). $\int C_i(t) Q_i(t)$ is the mass between time t_i and t_{i+1} [M], $\int C(t) Q(t) dt$ is the total mass [M].

The mass flux of the MPs, TU, and Cl were cross correlated to identify the relationship among spring signals using a cross correlation function (CCF; where a good correlation was implied when a correlation coefficient R2 is between 0.7-1 and a lag correlation of 0).

4.3.7 Calculation of number of inhabitants using specific medical products

The number of consumers of specific persistent products per day can be calculated for each separate sub-catchment or for the entire upper catchment during various flow periods to estimate wastewater loads discharging into the river using the following. A similar approach was used by Buerge et al. (2006) to estimate the number of caffeine consumers.

$$N_{cap} = \frac{(C_{MP} Q_{MP})}{(CDR_{MP} R_{MP})} \quad \text{Equation 8}$$

Where the product $C_{MP} Q_{MP}$ is the daily mass flux in [M/T], R_{MP} is the percent release from the body to the environment [-]; CDR_{MP} is the consumption rate per day in [M/T] and N_{cap} is the number of MPs' consumers, and 86400 is the number of seconds in a day.

CHAPTER

5. RESULTS

5.1 Tracer tests

5.1.1 *Nahr el Kalb River*

In February, 2016, the first arrival of Uranine during the Tracer tests conducted in the River was observed after about 2.8 hours from injection over a distance of 8240 m. This is equivalent to a maximum velocity of 0.88 m/s, very typical of surface water. The breakthrough curve reveals two peaks (Figure 5-1). Table 5-1 shows maximum concentrations and time of peak concentrations.

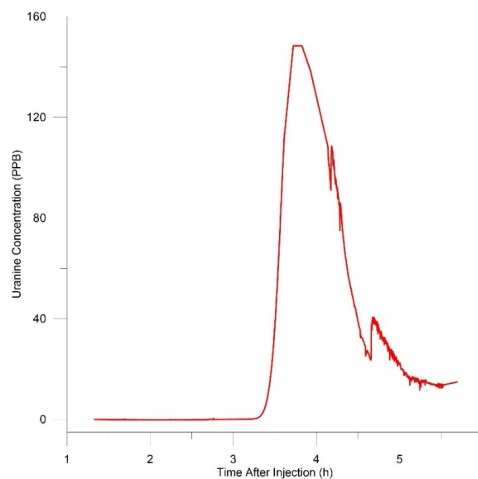


Figure 5-1. Figure showing Feb dye River TBC

5.1.2 *Qachqouch Spring*

The injected tracer was recovered in Qachqouch spring in the three tracer experiments, where each breakthrough curve was characterized by three distinct peaks. The Uranine was first detected at the spring 6.75 hours, 8.3 hours, and 20 hours after injection with maximum velocities estimated at 0.36 m/s, 0.19 m/s, 0.12 m/s for November Dye, February Dye, and May Dye respectively (Figure 5-2, table 5-1).

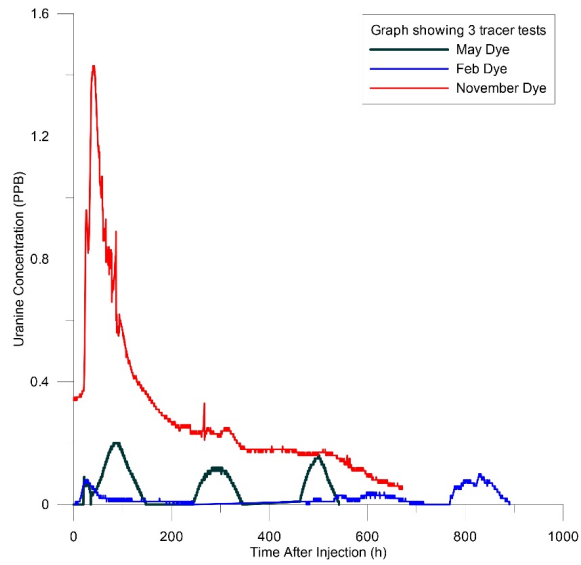


Figure 5-2. TBC of all tracer tests

		Peak Start (h)	Peak End (h)	Concentration Time (h)
Peak 1	May Dye 1	19	35	15
	May Dye 2	35	147	112
	Feb Dye	13	58	45
	November Dye 1	6.7	29.5	23
	November Dye 2	29.7	117.5	88
Peak 2	May Dye	241	344	103
	February Dye 1	481	508	27
	February Dye 2	526	560	34
	February Dye 3	586	708	122
	November Dye	299	334	35
Peak 3	May Dye	461	542	81
	February Dye	768	819	51
	February Dye 2	823	890	67
	November Dye 1	450	559	109
Peak 1	Surface water	2.8	4.6	1.8
Peak 2		4.6	5.6	1

Table 5-1. Table showing graphical parameters of TBC.

5.2 Micropollutant results

The MPs detected in the two campaigns, especially in locations NK6 and NK7 close to the River outlet were:

- 1) Analgesics and anti-inflammatory drugs such as; Acetaminophen (ACET), Diclofenac (DIC), Ibuprofen (IBU), Ketoprofen (KET), Meclofenamic Acid (MeAc), and Naproxen (NAP)
- 2) Anti-convulsant such as Carbamazepine (CBZ)
- 3) Antibiotics such as Amoxicillin (AMO)
- 4) Pain reliever and fever reducer such as Dilantin (DIL) and Meprobamate (MEP)
- 5) Lipid regulator such as Gemfibrozil (GEM)
- 6) Steroids and hormones such as Estradiol (ESD) and Estriol (EST)
- 7) Ulcer treatment such as Cimetidine (CIM), β -blocker such as Atenolol (ATE)
- 8) Veterinary drug such as Carbadox (CBX)
- 9) Contrast media such as Iohexol (IOX) and Iopromide (IOP)
- 10) Nervous stimulants such as 1,7-Dimethylxanthine, Caffeine (CAF), Theophylline (TEP), Theobromine (TEB)
- 11) Artificial sweeteners such as Acesulfame-k (ACE-K) and Sucralose (SUC)
- 12) Tobacco product Cotinine (COT)
- 13) Anti-bacterial and surfactants such as Triclocarban (TRI) and Nonylphenol, (NON) Quinolin (QUI)
- 14) Industrial waste such as the fire retardant TCEP, the herbicide 2,4,D, plasticizer BPA.

In this section, concentration and mass fluxes of selected micropollutants occurring ubiquitously and frequently on the catchment area will be discussed. Mass fluxes (in g/d) in

addition to concentrations (ng/l) were used in the analysis to account for the effect of river dilution in the estimation of loads.

5.2.1 Campaign 1: 2015

During the first campaign (2015), one of the three tributaries of the River (RIII) runs dry at the end of the snow melting season (River discharge ranging between 1.5 and 1.8 m³/s; Qachqouch spring discharge was at a mean of 0.7 m³/s). IOX, GEM, ACE-K, and IBU are found in all the samples collected along the River at variable concentrations in ng/l (Table 5-2, figure 5-3).

In Sub-catchment I, mass loads of ACE-K, GEM, IBU and IOX reached by increasing order of occurrence 7.60, 2.16, 1.64, and 1.47 g/d respectively, while the mass fluxes of the latter MPs were estimated at 2.33, 0.35, 0.43, 0.26 g/d in Sub-catchment II respectively. Additionally, the surfactant TRI was detected in Sub-catchment I (0.69 g/d).

On the main River, downstream to the two tributaries I and II, the mass loads of MPs of ACE-K, IBU, and IOX decrease or remain constant, while the mass loads of GEM and TRI increase drastically, downstream to the chicken farm, indicating a considerable inflow of concentrated wastewater. About 7000 m downstream of NK3-0, most of the MPs decrease except IBU and ACE-K. They increase simultaneously reaching mass loads of 16.5 g/d and 2.5 g/d respectively.

It is worth noting that the mass input of other MPs such as CAF and ACET (with relatively low half-lives; <15 days; Buerge et. al 2003; Lin et. al 2010) increases over the last 7000 m of the River as well, indicating perennial domestic wastewater effluents along the River. EST is occasionally detected downstream to the chicken farm.

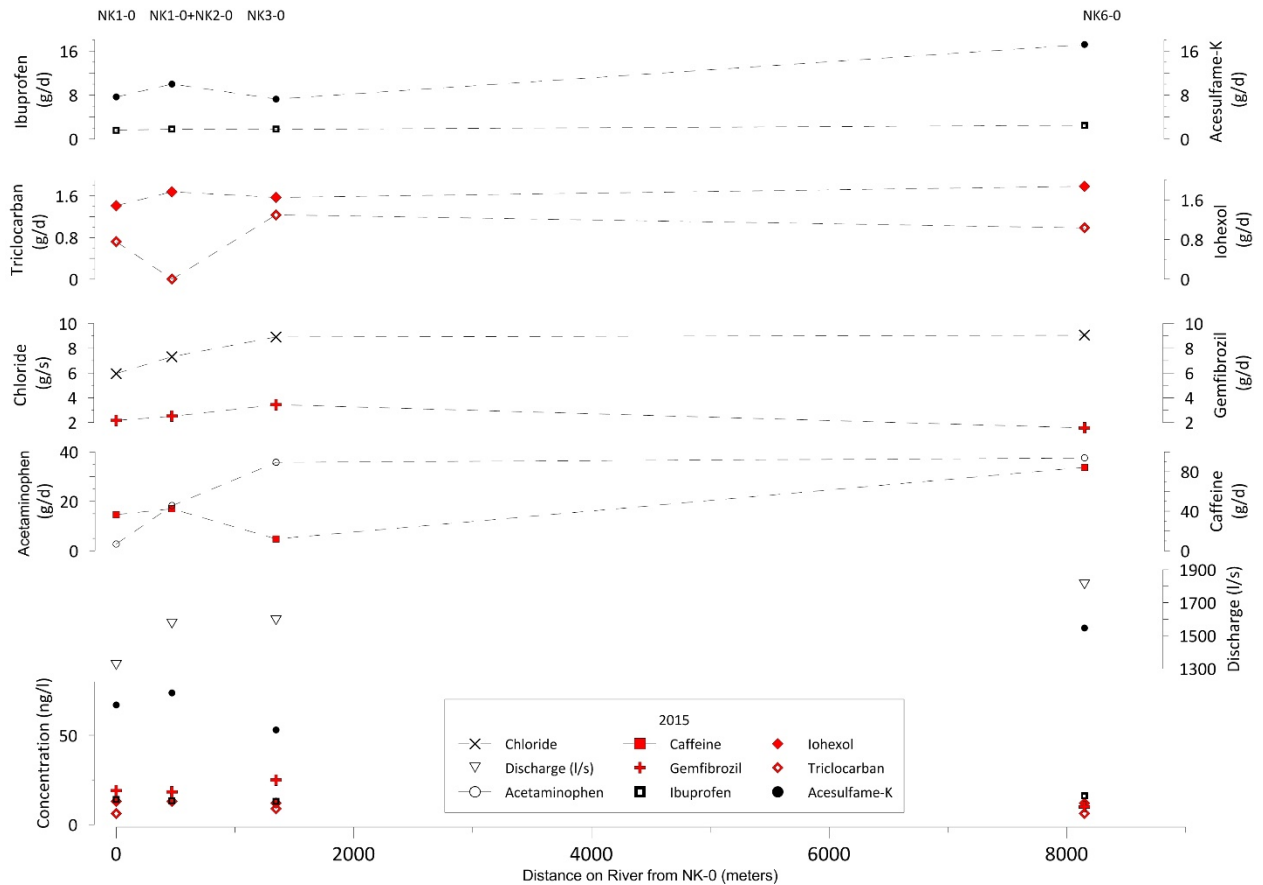


Figure 5-3. Variation of concentrations and daily mass fluxes of selected MPs, and chloride along the River from first sample (NK1-0 0 m)

Unlike IBU, ACE-K was found in the two sampled wells and the Qachqouch spring at concentrations ranging between 170-640 ng/l. TRI was detected in the springs ABM and Qachqouch and the two sampled wells at concentrations around 6-7 ng/l. IOX was detected in one well and the Qachqouch and ABM springs at concentrations of 12-13 ng/l. Other substances such as SUC were found exclusively in the Qachqouch spring (Table 5-3). In the wastewater sample on the lower catchment (Flow around 0.01 l/s), the following substances were reported: 1) ACE-K, SUC at concentrations of 210000 and 760 ng/l respectively, 2) COT at concentrations of 7100 ng/l, and 3) ACET and IBU at concentrations of 7200 and 2100 ng/l. It is worth noting that CAF and DIC were not found in wastewater.

Samples	Units	MRL (ng/l)	Error (%)	Sub-catchments		Main	
				II NK 2-0	I NK 1-0	I and II NK4-0	I+II downstream NK 6-0
Sampling Date				6/5/2015	6/3/2015	6/4/2015	6/5/2015
Flow (±10%)	l/s			250	1323	1592	1810
Time				11:15	10:00		13:40
Analysis				6/16/2015			
Gemfibrozil	ng/l g/d	5	7	15 0.3	19 2.2	25 3.4	10 1.6
Iohexal	ng/l g/d	10	22	13 0.3	13 1.5	0 0.0	12 1.9
Acesulfame-K	ng/l mg/s	20	0	110 2.4	67 7.7	53 7.3	110 17.2
Ibuprofen	ng/l g/d	10	6	10 0.2	14 1.6	13 1.8	16 2.5
Diclofenac	ng/l g/d	5	4	9 0.2	10 1.1	0 0.0	8 1.3
Acetaminophen	ng/l g/d	5	34	24 0.5	720 82.3	260 35.8	240 37.5
Atenolol	ng/l g/d	5	1	5 0.1	12 1.4	0 0.0	6 0.9
Caffeine	ng/l g/d	5	2	270 5.8	320 36.6	87 12.0	540 84.4
Cotinine	ng/l g/d	10	11	20 0.4	31 3.5	18 2.5	21 3.3
Triclocarban	ng/l g/d	5	6	0 0.0	6 0.7	9 1.2	6 0.9
Theophylline	ng/l g/d	20	48	32 0.7	0 0.0	0 0.0	0 0.0
Amoxicillin	ng/l g/d	20	4	0 0.0	220 25.1	0 0.0	0 0.0
Iopromide	ng/l g/d	5	4	6 0.1	0 0.0	0 0.0	0 0.0
Estriol	ng/l g/d	5	4	0 0.0	0 0.0	70 9.6	6 0.9
Cimetidine	ng/l g/d	5	3	0 0.0	0 0.0	0 0.0	900 140.7
Dilantin	ng/l g/d	20	33	0 0.0	0 0.0	0 0.0	180 28.1
Meprobamate	ng/l g/d	5	20	0 0.0	0 0.0	0 0.0	100 15.6
Quinoline	ng/l g/d	5	5	0 0.0	0 0.0	0 0.0	14 2.2
Salicylic acid	ng/l g/d	100	5	0 0.0	0 0.0	0 0.0	2000 312.8

A value of 0 implies BMRL= Below Mean Reporting Limit

Table 5-2. Concentrations and mass fluxes of sampled micropollutants for campaign I.

Samples	Units	MRL (ng/l)	Error (%)	Qachqouch					Wells			WW
				Q1-2	Q1-3	Q1-4	Q1-5	Q1	ABM	H1	AK1	BC1
Sampling date				30/12/16	2/01/16	5/01/16	7/01/16	5/5/2015	5/5/2015	5/5/2015	5/5/2015	5/5/2015
Flow (±10%)	l/s		8	300	1300	7500	2900	700	-	-	-	-
Time				20:00	4:00	20:00	20:00	18:00				
Analysis				30/01/2017				6/16/2015				
Nonylphenol	ng/l	100	30.5	490	310	180	310	0.0	0	0	0	0
	g/d			12.70	34.82	116.64	200.88	0.00	N/A			
Gemfibrozil	ng/l	5	6.2	0	5.2	38	9.3	0	0	0	0	3500
	g/d			0.00	0.58	24.62	6.03	0.00	N/A			
Iohexal	ng/l	10	8.2	19	0	47	0	12.0	13	13	0	290
	g/d			0.49	0.00	30.46	0.00	0.73	N/A			
Acesulfame	ng/l	20	3.1	78	120	200	94	170.0	0	180	640	210000
	g/d			2.02	13.48	129.60	60.91	10.28	NA			
Sucralose	ng/l	100	9.0	120	210	150	260	120.0	0	0	0	760
	g/d			3.11	23.59	16.85	168.48	7.26	N/A			
Triclocarban	ng/l	5	6.0	0	0	0	0.25	7.1	6.10	6.50	6.10	0
	g/d			0.00	0.00	0.00	0.16	0.43	N/A			
Ibuprofen	ng/l	10	6	0	0	0	0	0	0	0	0	2100
Caffeine	ng/l	5	2	NA	NA	NA	NA	0	0	0	0	0
Cotinine	ng/l	10	11	NA	NA	NA	NA	0	0	0	0	7100
Acetaminophen	ng/l	5	34	NA	NA	NA	NA	0	0	0	0	7200

Table 5-3. Concentrations of micropollutants in groundwater and wastewater samples collected in campaign I (2015) and in 2016.

A value of 0 implies BMRL= Below Mean Reporting Limit

NA: Not Analyzed

N/A: Not Applicable

5.2.2 Campaign 2: 2017

Out of the 29 sampled PPCPs, only IBU, GEM, IOX, and ACE-K were detected frequently in the seven samples due to the high dilution from snowmelt. A greater range of MPs was found in two samples (NK-4 and NK-7). The concentrations and mass fluxes of the different compounds are shown in table 5-4 and figure 5-4.

In sub-catchment I, the detected micropollutants are NON (190 ng/l), GEM (33 ng/l), and IOX (75 ng/l). This constitutes an equivalent load of 28.5 g/d, and 5.1 g/d and 8.64 g/d of these three MPs respectively. In sub-catchment II, the micropollutants are NON (110 ng/l) and GEM (24 ng/l), equivalent to MPs' mass loads of 10.4 g/d and 2.6 g/d respectively. GEM (140 ng/l, mass flux 14.7 g/d) NON (140 ng/l, mass flux 14.7 g/d), IBU (200 ng/l, mass flux 21.6 g/d) and ACE-K (300 ng/l, mass flux 32.8 g/d) were found in the sample collected in NK3 (RIII).

In the four samples taken along the River NK4, NK5, NK6, and NK7, GEM is detected at all times with concentrations varying between 16-54 ng/l and mass loads between 5.2 and 22 g/d. ACE-K and IBU are found simultaneously in NK4 below point sources contaminations and at the last sampled location on the River (NK7) at concentrations of 160 and 200 ng/l. IOX is also observed in most of the samples along the river at concentrations of 20-75 ng/l. equivalent to daily mass loads of 8.6-26 g/d. Finally, the surfactants such as TRI (MLR of 5 ng/l), reported in campaign I was absent in samples of campaign II. *Fecal coliform* and *enterococci* concentration and fluxes increase along the River with increasing chloride mass loads (from wastewater effluents) in places. (Figure 5-4)

Samples	nits	MRL (ng/l)	Error (%)	Tributaries/sub-catchment			Main			
				I	II	III	I and II	I II and III		
				NK1	NK2	NK3	NK4	NK5	NK6	NK7
Sampling date				30/03/2017				31/03/2017		
Flow (±8%)	l/s		8	1755	1097	1239	2907	4021	4544	4800
Time				14:33	14:45	15:20	17:00	12:30	16:30	18:00
Analysis				20/04/2017	20/04/2017	20/04/2017	25/04/2017	20/04/2017	20/04/2017	25/04/2017
Nonylphenol	ng/l	100	30.5	190	110	140	110	150	0	100
	g/d			29	10	15	28	52	0	41
Gemfibrozil	ng/l	5	6.2	33	24	140	20	16	54	41
	g/d			5	2	15	5	6	21	17
Iohexal	ng/l	10	8.2	75	0	0	0	75	60	20
	g/d			11	0	0	0	26	24	8
Acesulfame-K	ng/l	20	3.1	0	0	310	51	0	0	200
	g/d			0	0	33	13	0	0	83
Ibuprofen	ng/l	10	9.0	0	0	200	85	0	0	160
	g/d			0	0	21	21	0	0	66
Iopromide	ng/l	5	22.2	5.1	0	0	0	0	0	0
BPA	ng/l	5	5.1	0	0	15	0	0	0	0
Diclofenac	ng/l	5	4.8	0	0	23	0	0	0	15
Estriol	ng/l	5	3.8	0	0	5.4	0	0	0	0
Naproxen	ng/l	10	4.0	0	0	25	0	0	0	16
2,4 D	ng/l	5	2.4	0	0	40	0	0	0	92
Sucralose	ng/l	100	7.4	0	0	0	0	0	150	0
Salicylic acid	ng/l	100	10.0	0	0	7200	0	0	0	0
Substances measured in samples NK3 and NK7										
Caffeine	ng/l	5	1.5	NA	NA	NA	220	NA	NA	440
Cotinine	ng/l	10	5.1	NA	NA	NA	22	NA	NA	72
Theophylline	ng/l	20	3.7	NA	NA	NA	22	NA	NA	58
Theobromine	ng/l	10	8.6	NA	NA	NA	110	NA	NA	230
Amoxicillin (semi-quantitative)	ng/l	20	4.4	NA	NA	NA	32	NA	NA	72
Carbamazepine	ng/l	5	0.1	NA	NA	NA	NA	NA	NA	7.9
Atenolol	ng/l	5	6.7	NA	NA	NA	NA	NA	NA	13
Carbadox	ng/l	5	1.3	NA	NA	NA	NA	NA	NA	12
Ketoprofen	ng/l	5	0.6	NA	NA	NA	NA	NA	NA	5.8
Meclofenamic Acid	ng/l	5	3.8	NA	NA	NA	NA	NA	NA	16
Acetaminophen	ng/l	5	3	NA	NA	NA	510	NA	NA	1000
A value of 0 implies BMRL= Below Mean Reporting Limit										
NA: Not Analyzed										

Table 5-4. Concentrations and mass fluxes of sampled micropollutants and major ions for campaign II.

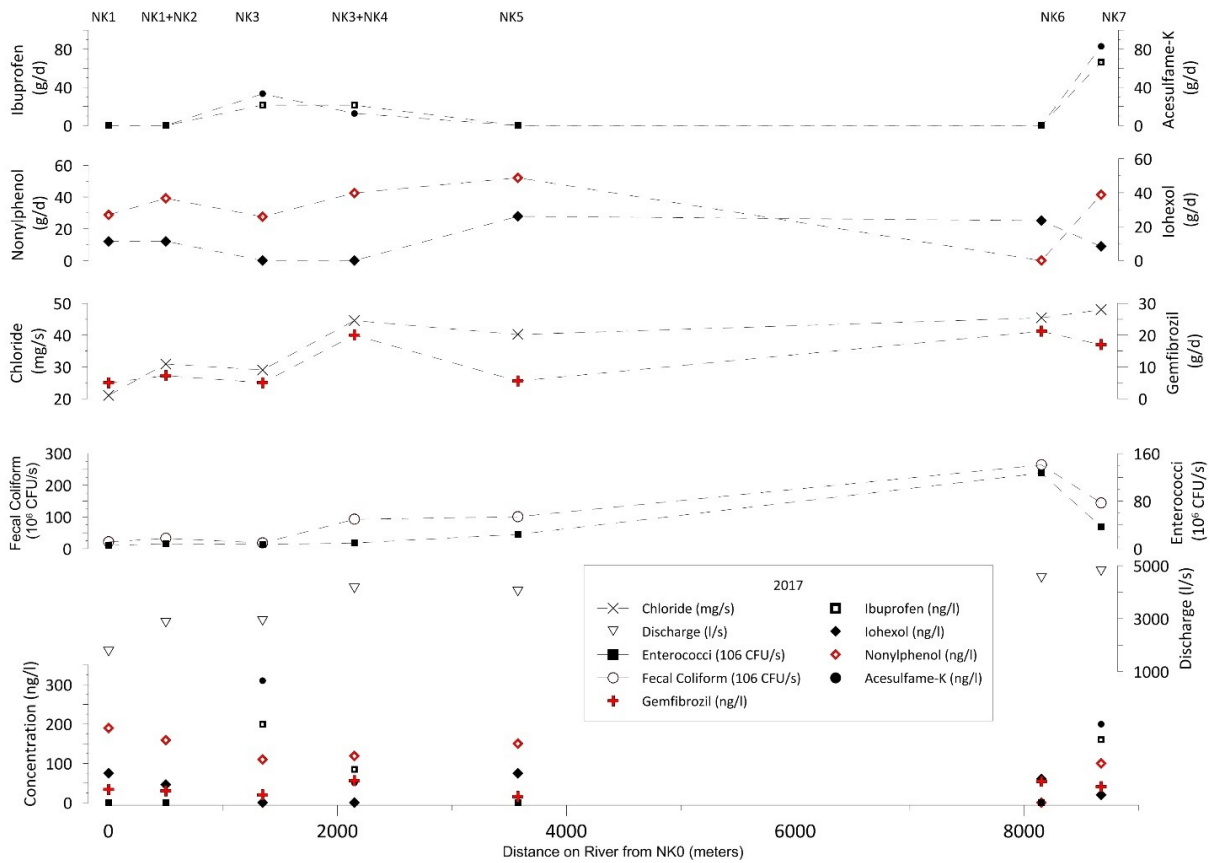


Figure 5-4. Variation of concentrations and mass fluxes of selected MPs, chloride, *fecal coliforms* and *enterococci* along the River from first sample (NK1 0 m)

5.3 Occurrence of specific MPs

ACE-K and IBU mass fluxes correlate very well on surface water during both campaigns, indicating a similar origin of both MPs and probable combined use in the same medicine (Jeppson et al., 2016; Figure 5-5). The mass fluxes of ACE-K in all samples slightly increased since 2015. Mass fluxes of IBU are significantly higher in recent campaign by approximately 10 folds when found.

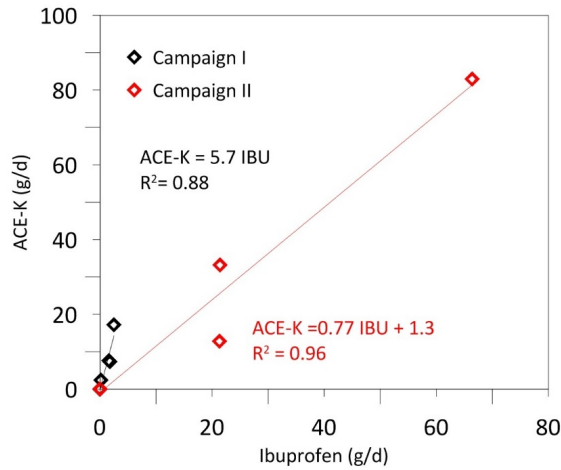


Figure 5-5. Correlation between mass fluxes of ACE-K and IBU indicating their co-existence in specific medicine

GEM mass loads on the catchment increased by a factor of 1.5-2 in the upper sub-catchments since 2015 from a total of 5.3 to 7.7 g/d.

The mass loads of ACE-K and GEM in the Qachqouch spring increase linearly with increasing discharge (Figure 5-6); ACE-K mass fluxes in the spring vary in low and high flow periods between 2.02 g/d and 130 g/d while those of GEM varies between 0 and 24.6 g/d.

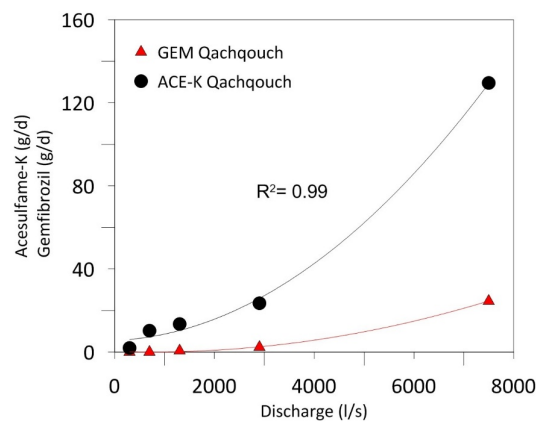


Figure 5-6. Correlation between ACE-K mass flux in the Qachqouch spring and its discharge rate

5.4 Event Results

Following the four monitored precipitation events, four spring responses with varying peak discharges were detected (characteristics of the spring responses in the four events are summarized in table 5-5 and figure 5-7). The pre-event flow rate was 0.29 m³/s; during the events, the maximum discharge at the spring varied between 2.0 and 11 m³/s, with total discharged volumes ranging between 0.3 Mm³ to 4 Mm³. The higher the response time at the spring (with respect to start of rain event), the lower the percentage of newly infiltrated waters, indicating a lower transit time of phreatic or diffuse waters.

Newly infiltrated waters during the three events constituted between 3.0% and 24 % from the total discharged volume. In every spring response, a turbidity peak was observed simultaneously with a decrease of Cl concentrations indicating newly infiltrated waters arriving at the spring. In the third event two turbidity peaks were discerned; a primary peak and a secondary peak attributed to a sinking river (Figure 5-7; River flood level exceeds baseline level). Depletion in Deuterium (²δH) and heavy Oxygen (¹⁸δO) accompanied the first turbidity peaks in all of the events, whereas enrichment in the heavy stable isotopes was observed with the secondary turbidity peak.

Out of the 27 tested MPs, only five were detected in all of the samples (including GEM, IOX, SUC, ACE-K, and the cleaning agent 4-nonylphenol) possibly due to the high dilution effect. It is worth mentioning that substances characterized by a relatively short half-life such as diclofenac and ibuprofen were below detection limits (5 and 10 ng/l respectively).

	P (mm)	Response lag ($t_{s0}-t_{p0}$) (hours)	Q_{max} (m^3/s)	V_n ; (Mm ³) % of V_T	V_i ; (Mm ³)	C_{max} (ng/l) [SUC]; [ACE-K]	C_{max} (ng/l) [GEM]; [IOX]	New Mass (g) SUC; ACE-K	Total Mass (g) SUC; ACE-K	New Mass (g) GEM; IOX	Total Mass (g) GEM; IOX
Event 1 (E1)	53	12.5	2.05	0.01-3.0%	0.27	300; 180	16; 18	28; 14	58; 34	1.00; 0.46	2.04; 1.95
Event 2 (E2)	33	19.0	2.95	0.01 –3.4%	0.29	290; 150	9.5; 12	10; 7.0	70; 40	0.64; 0.00	1.72; 1.08
Event 3 (E3)	29	4.50	10.8	0.36-24%	1.56	320; 200	38; 47	55; 74	302; 242	24.0; 15.0	29.0; 24.0
River (E3)	-	-	7.97	0.1-6.4%	1.56	150; 200	38; 47	0.0; 37	302; 242	13.4; 13.0	29.0; 24.0
Event 4 (E4)	53	6.00	9.80	0.2- 5%	4.00	NA		NA	NA	NA	NA

T_{p0} = Time since precipitation started

T_{s0} = Time of first response

V_n =Total volume of newly infiltrated waters

V_i =Total volume of water per event

Table 5-5. Summary of the spring response to the monitored events in terms of time to response, volumes of rapid infiltrated water, total volumes, percent of new volume to total volume, mass loads of SUC, ACE-K,GEM, and IOX in the spring

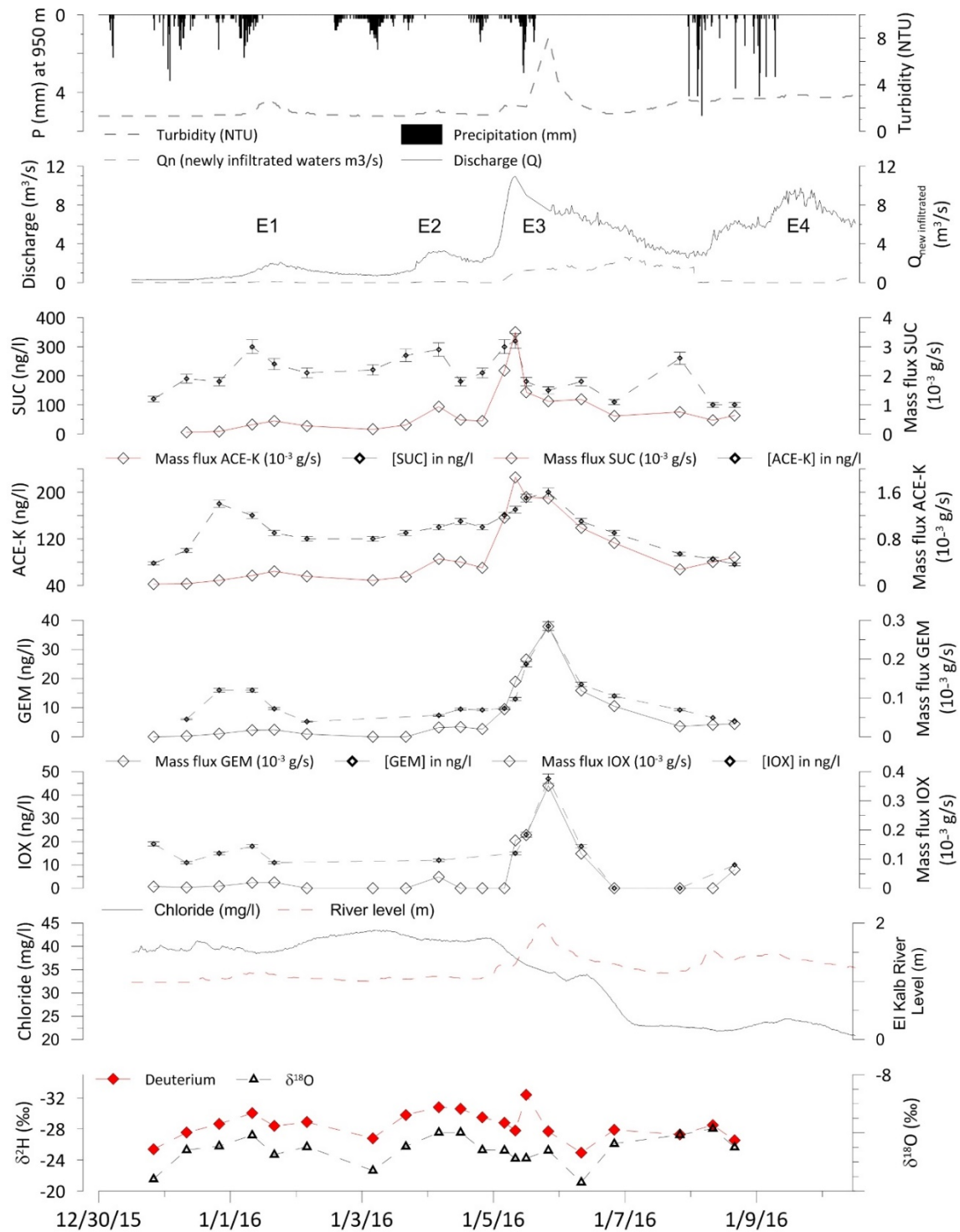


Figure 5-7. Chemograph showing the variation of physico-chemical parameters and concentrations and mass fluxes of investigated micropollutants as a response to three consecutive precipitation events (E1 to E3; 15-min precipitation data). E1 to E4 refer to the four consecutive occurring events”.

The four investigated MPs (SUC and ACE-K, GEM and IOX) were found in the pre-event waters at concentrations 120, 78.0, 6.10, and 19.0 ng/l, equivalent to mass fluxes of 0.035 0.023, 0.002, 0.003 (10^{-3} g/s) respectively. In the first three events, three different breakthrough of the artificial sweeteners ACE-K, SUC, Gem, and IOX can be observed (Figure 5-7). Maximum concentrations of SUC varied in the three events between 290-320 ng/l, while that of ACE-K varied between 150-200 ng/l. The total mass of ACE-K and SUC arriving at the spring in the three events is shown in table 5-5; reaching 316 and 430 g of ACE-K and SUC respectively. Similarly, three distinct breakthrough curves of IOX and GEM can be observed in the spring multi-response (Figure 5-7 and table 5-5). The major increase of mass flux for GEM and IOX occurs during the third event along with the secondary turbidity peak, while that of the ASWs occurs with the primary turbidity peaks.

In the three events about 10- 32 g of SUC and 7-15 g of ACE-K arrived with fast infiltrated waters with the primary turbidity peaks through fast pathways to the spring. During event 3, an additional amount of 37 g of ACE-K was introduced by infiltration from the river, while 0 grams of SUC (out of a total of 55 g) arrived to the spring with the secondary turbidity peak.

During the three events, 1.0-24 g of GEM and 0.5-15 g of IOX were estimated at the spring. No more than 1.5 g of IOX and 3.5 g of GEM arrived with the first three primary peaks. The significant load of around 13 g of IOX and GEM coincided with the secondary turbidity peak in the third event.

Concentrations of SUC and ACE-K detected at the springs are not well synchronized in the observed breakthrough curves as shown in (Figure 5-7). Moreover, EC and Cl concentrations do not correlate well with the ASWs, GEM, or IOX (Figure 5-8).

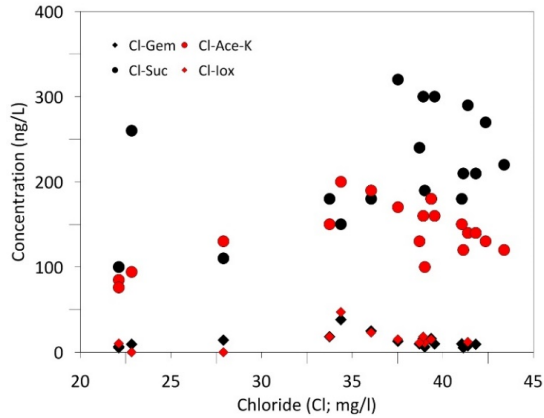


Figure 5-8. Correlation between concentrations of the four MPs (ACE-K, SUC, GEM, IOX) and Chloride showing that the breakthrough of the four MPs is not simultaneous at the spring at all times.)

Nevertheless, the breakthrough curves of mass fluxes (Q_i [C_i]) of ASWs are very well correlated with primary turbidity peaks in each of the events, except for the secondary turbidity. A maximum correlation between ASWs and TU ($R^2=0.99$ for ACE-K and $R^2=0.97$ for SUC) and ASWs and Cl mass fluxes (SUC $R^2=0.99$ to ACE-K $R^2=0.97$) is observed a time lag=0; Table 5-6; Figure 5-9). However, the other MPs mass fluxes correlate with those of Cl and TU with a lag time equals to -1 (Table 5-6; Figure 5-9). A negative lag indicates that the predictand precedes the predictor by one lag (equivalent to 4-8 hours).

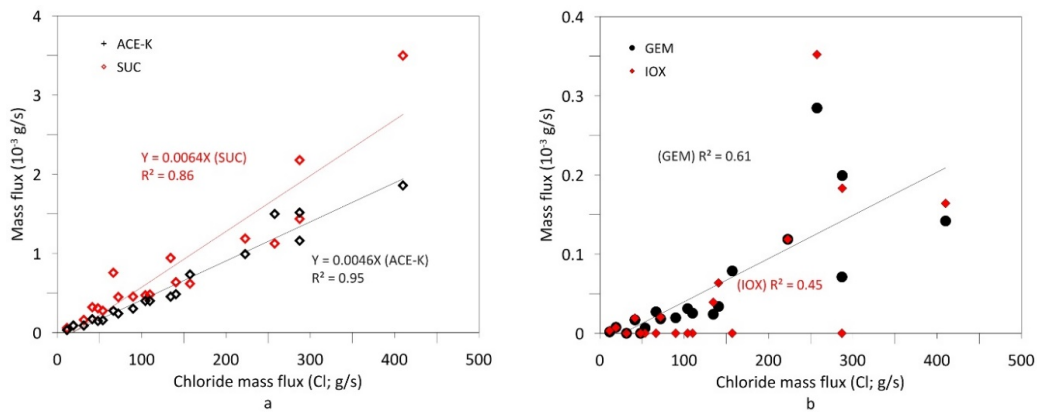


Figure 5-9. Correlation between mass fluxes of Chloride and mass fluxes of a) SUC and ACE-K and b) IOX and GEM in each of the three events.

		Predictor (mass fluxes; CQ)					
		GEM	IOX	SUC	ACE-K	TU	Cl
	GEM	1	0.92 (0)	0.96 (1)	0.96 (1)	0.95 (1)	0.95 (1)
	IOX	0.92 (0)*	1	0.92 (1)	0.91 (1)	0.92 (1)	0.89 (1)
	SUC	0.96 (-1)	0.92 (-1)	1	0.94 (0)	0.97 (0)	0.97 (0)
	ACE-K	0.96 (-1)	0.91 (-1)	0.94 (0)	1	0.99 (0)	0.99 (0)
	TU	0.95 (-1)	0.92 (-1)	0.97 (0)	0.99 (0)	1	0.99 (0)
	Cl	0.95 (-1)	0.89 (-1)	0.97 (0)	0.99 (0)	0.99 (0)	1

*Coefficient of correlation R^2 (lag time between predictand and predictor for a maximum R^2)

Table 5-6. Maximum cross correlation coefficient between the various spring signals (mass fluxes_ obtained for correlation lag times between predicand and predictor. One positive lag indicates that the predictand lags the predictor by one lag.

ACE-K and SUC mass fluxes are less correlated with those of GEM while they poorly relate to IOX. Despite a lower ratio of ACE-K to SUC in the wastewater sample, the ratio of ACE-K to SUC consumption during the three events on the catchment is 0.77 (Figure 5-10), indicating higher loads of SUC with respect to ACE-K and a possible similar origin of both compounds except when the origin is infiltrated surface water. The relationship between of GEM and IOX mass loads at the spring during the different events can be described linearly by $GEM = 0.86 [IOX] + 1.19$ ($R^2 = 0.97$; Figure 5-11), because IOX can decrease to below detection limits in the spring.

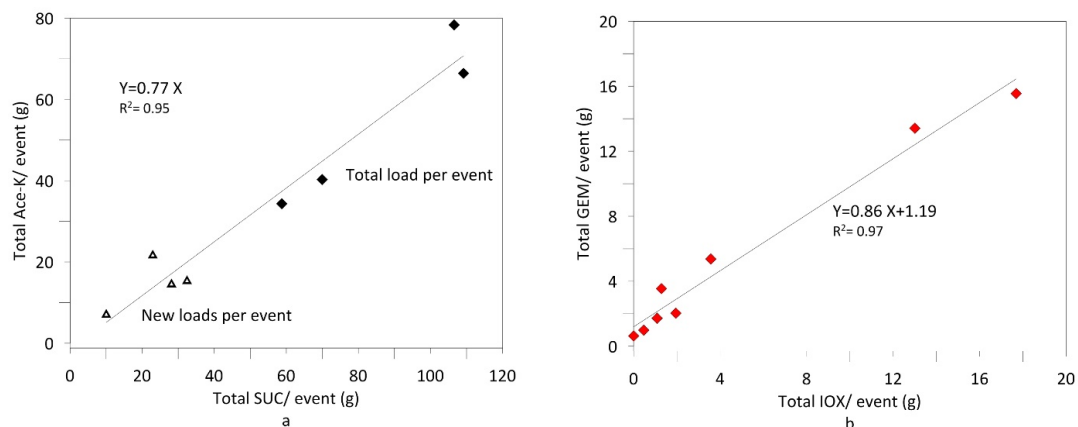


Figure 5-10. Linear correlation between total and additional mass loads of a) SUC and ACE-K, ratio= 0.77.b) GEM and IOX ratio =0.86.

Furthermore a relationship was established between new masses of GEM, IOX, and ACE-K, introduced to the spring and the total mass of each MP calculated in each event (Figure 5-11). The latter was less applicable in the case of SUC.

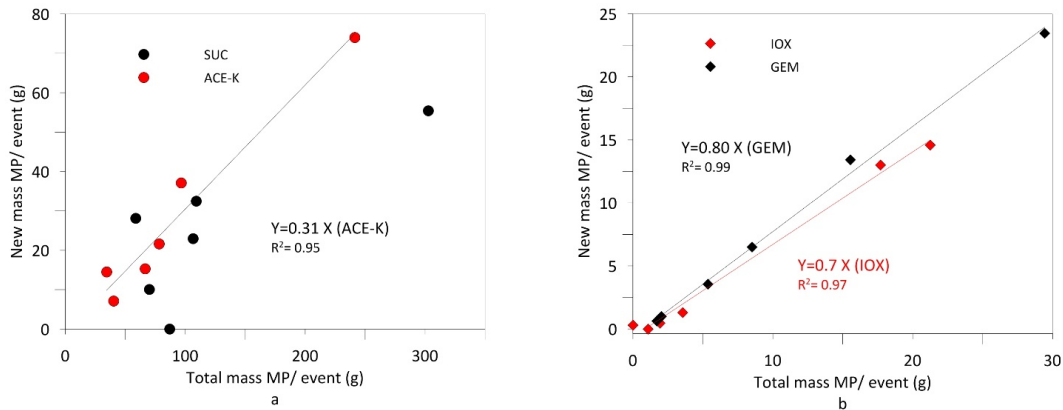


Figure 5-11. Correlation between total mass and newly introduced masses of each of the investigated MP per event showing a relationship between the new masses arriving through fast flow pathways and total masses calculated at the spring.

The variance of MPs breakthrough curves with respect to a mean transit time in events 1 and 2 was evaluated:

$$\sigma^2 = \frac{(t_i - t_m)^2 C_i(t) Q_i(t)}{\int C(t) Q(t) dt}; \text{ Figure 5-12.}$$

As a result, the variance of ACE-K breakthrough curve with respect to a mean transit time is slightly higher ($\sigma^2=0.71$ and 0.16 h^2) than that of SUC ($\sigma^2=0.68-0.16 \text{ h}^2$), TU ($\sigma^2=0.64-0.15 \text{ h}^2$), GEM ($\sigma^2=0.57-0.09 \text{ h}^2$), and IOX ($\sigma^2=0.31-0.07 \text{ h}^2$) respectively. Event 3 was excluded because of the secondary turbidity peak indicating a varying flux of ASWs from the River.

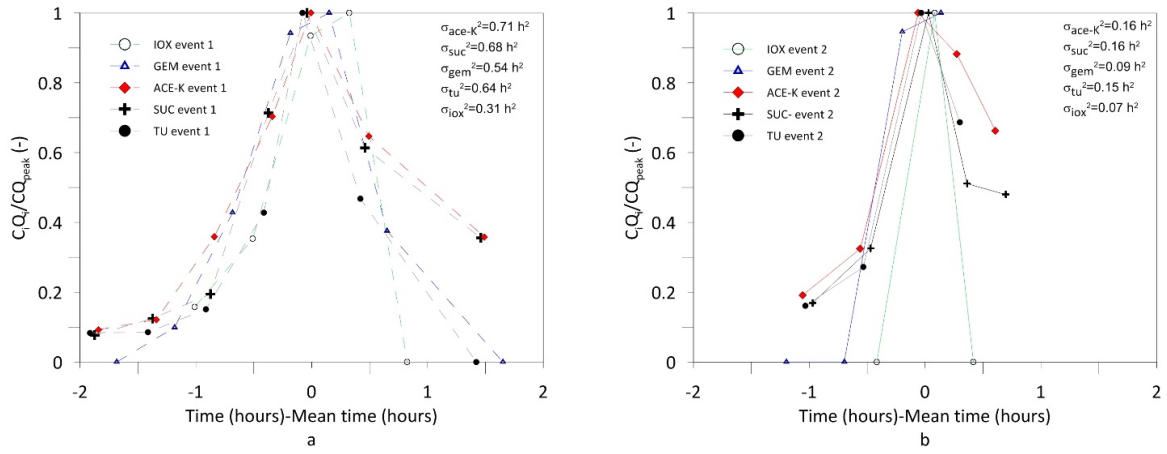


Figure 5-12. Comparison of the shape of normalized turbidity and MPs' mass flux C_iQ_i (with respect to peak mass flux $(CQ)_{max}$) as a function of normalized time (with respect to transit time; t_i-t_m) for the evaluation of the duration of MPs' retrieval at the springs for events 1 and 2

CHAPTER 6. DISCUSSION

6.1 Tracer tests

The main curve of the Green Dye experiment represents the water that traveled down the river and reached the fluorometer following a sinuous path, after a suspected percentage of that river water (along with the dye) infiltrated through the sinking stream into the groundwater networks. The resulting second peak could be evidence of the sinking stream, where water infiltrates into the ground and then emerges back out to the river. This delay is due to water traveling a longer path, slower than that of the riverbed. Moreover, Hauns et al. 2001, Massei et al. 2006, Morales et al. 2010 state that secondary peaks could also be attributed to tracer being trapped in eddies.

The fact that each tracer test on the Nahr el Kalb revealed breakthrough curves indicates the travel of tracer from the surface water to the groundwater system through permeable karst conduits. Each of the tracer tests showed three separate and distinct peaks, which according to Goldscheider et al. (2008) indicates a possible bifurcated flow path, i.e. three different conduits. Another interpretation of the multiple peak response could be by the presence of underground lakes (Dewaide et. Al 2018).

6.2 Quantification of wastewater discharge and concentration

Based on campaign 1 (medium to low flow), the wastewater discharge into the River was estimated between two consecutive points based on chloride variation, when inflowing wastewater contributed to the increase of chloride mass fluxes. In Campaign 1, it

varied between 0.9 and 10 l/s (0.3-2.0 % of inflowing pristine waters). The decrease is attributed to the drying out of one of the major flowing tributary (RIII) carrying wastewater from highly urbanized villages. Effluents during low flow periods may originate only from specific point source outlets close to the river. If it is assumed that wastewater reaches 150 l/capita per day, a total number of 9000 inhabitants are discharging WW into the River, while the rest might be discharged onto the groundwater catchment or through bottomless pits.

In campaign 2 (high flow), while all tributaries are active channels, the wastewater flow along the River ranged between 9.0 and 64 l/s. This flow consists of 2.0-5.0 % of the inflowing pristine waters in the River. In that case, it is estimated that 70,000 inhabitants are discharging WW into the River, divided into specific sub-catchments as follows (in capita): RII: 17,500, RIII: 36,900, and a total of 15,500 along the main River downstream to RIII).

6.3 MPs Concentrations and Frequency of Detection

In Campaign I, the MPs frequency of detection by increasing order is as follows: TRI< IBU< IOX<GEM<ACE-K. On the other hand, in campaign II the MPs occurrence by order of increasing magnitude is as follows: IOX<IBU<ACE-K<GEM<NON (semi-qualitative).

In wastewater, the occurrence of MPs increases as follows: IOX<IBU<GEM<ACE-K, with the absence of TRI and NON. While GEM falls below detection limits in most of groundwater samples, only ACE-K (170-640 ng/l), TRI (6-7 ng/l), and IOX (12-13 ng/l) are found in spring water and wells. The latter implies a variable distribution of MPs in both surface water and groundwater catchments. The higher frequency of occurrence is related either to a considerate usage of a compound, to its higher persistence in the system, or to specific point source contaminations (such as chicken farm, hospitals). Therefore, there is a

need to address the treatment of most persistent MPs especially in the future, with consumption and population increase.

IBU and ACE-K, highly correlated together, could be used as wastewater co-tracers for domestic wastewater (Liu et. al 2014), because of their similar origin. A lower ratio of IBU to ACE-K observed during low flow periods is probably due to a subsequent degradation of IBU in the stored old wastewater (Mersmann et. al, 2003; May 2015 compared to March 2017). Moreover according to Einsiedl et. al., (2010), sorption of IBU cannot be ruled out. Degradation of IBU and persistence of ACE-K (Brorström-Lundén et al, 2007; Mead et al, 2009; Perkola et al, 2014) in natural environments explains why ACE-K displays a higher mass flux than IBU in both campaigns.

TRI was detected in campaign 1 and absent in campaign 2, because of high dilution of snowmelt rather than its absence in WW effluents. On the other hand, the surfactant NON detected in the 2017 campaign and in 2016 spring waters may be due to the recent usage of NON-rich products on the catchment from hospital waste (Higuchi et al., 2004). Additionally, the absence of substances such as diclofenac and caffeine with a relatively low half-life span indicates that they would have decayed by the time of sampling in presumably old stored wastewater on the catchment.

Sub-catchments RI and RII, and RIII are the source of considerable mass loads of the selected MPs, which are thought to be discharged into the river by small streams on valley flanks. An increase of a mass flux implies either an addition of mass loads from hospital or domestic waste or from daughter metabolites. A decrease of the mass flux along the River implies a degradation of the compound. In 2017, mass fluxes of selected MPs such as IOX, GEM, ACE-K, and IBU, in addition to TRI and NON were compared to those of 2015 to detect variation in the consumption with time (Figure 6-1 and figure 6-2). Generally,

MPs' mass fluxes estimated in campaign II are greater than those of campaign I; this is due to either an increase in consumption, the higher amount of WW effluents coming from more settlements into the River, or by the diffusive infiltration from contaminated influent groundwater.

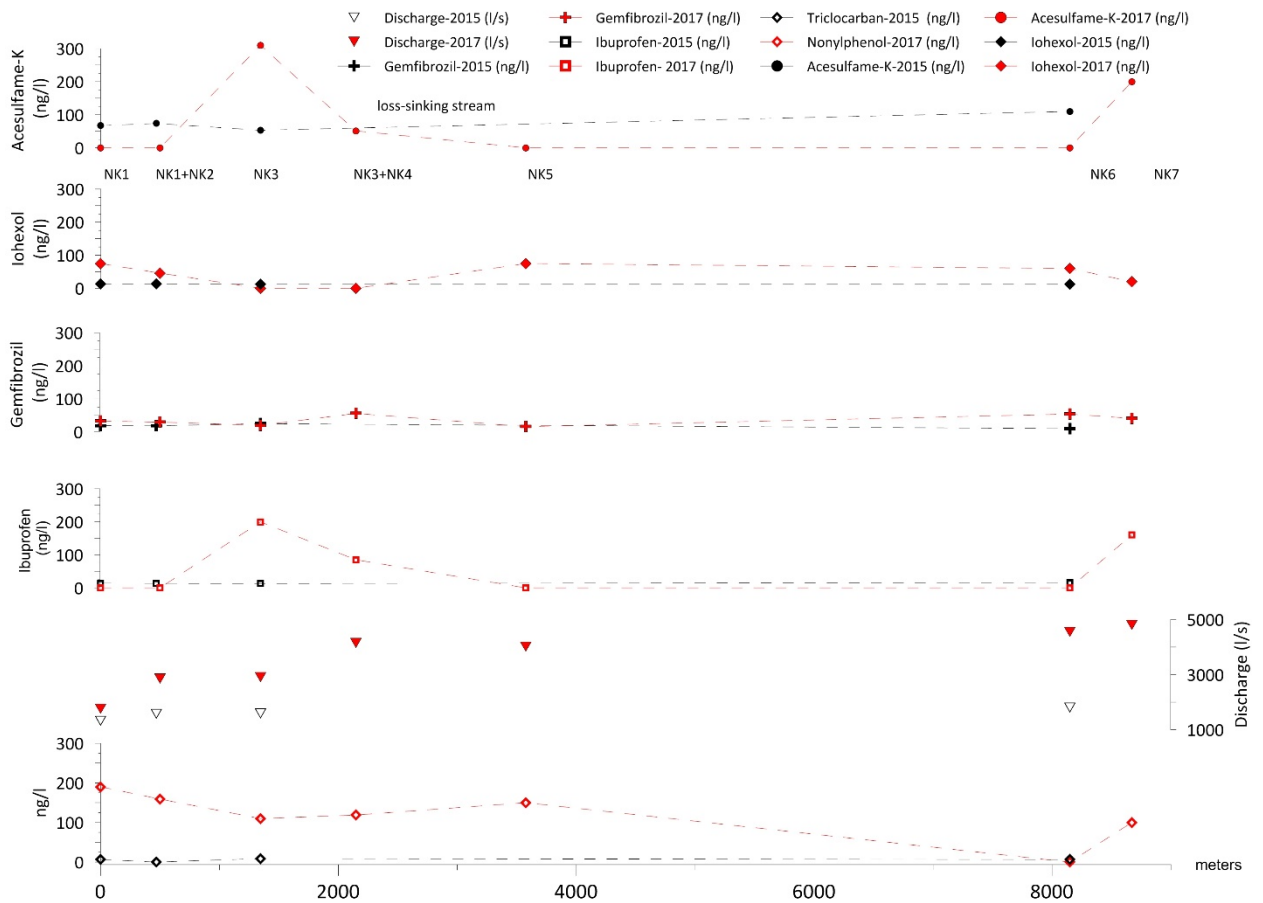


Figure 6-1. Comparison of variation of discharge and concentration of micropollutants in both sampling campaigns

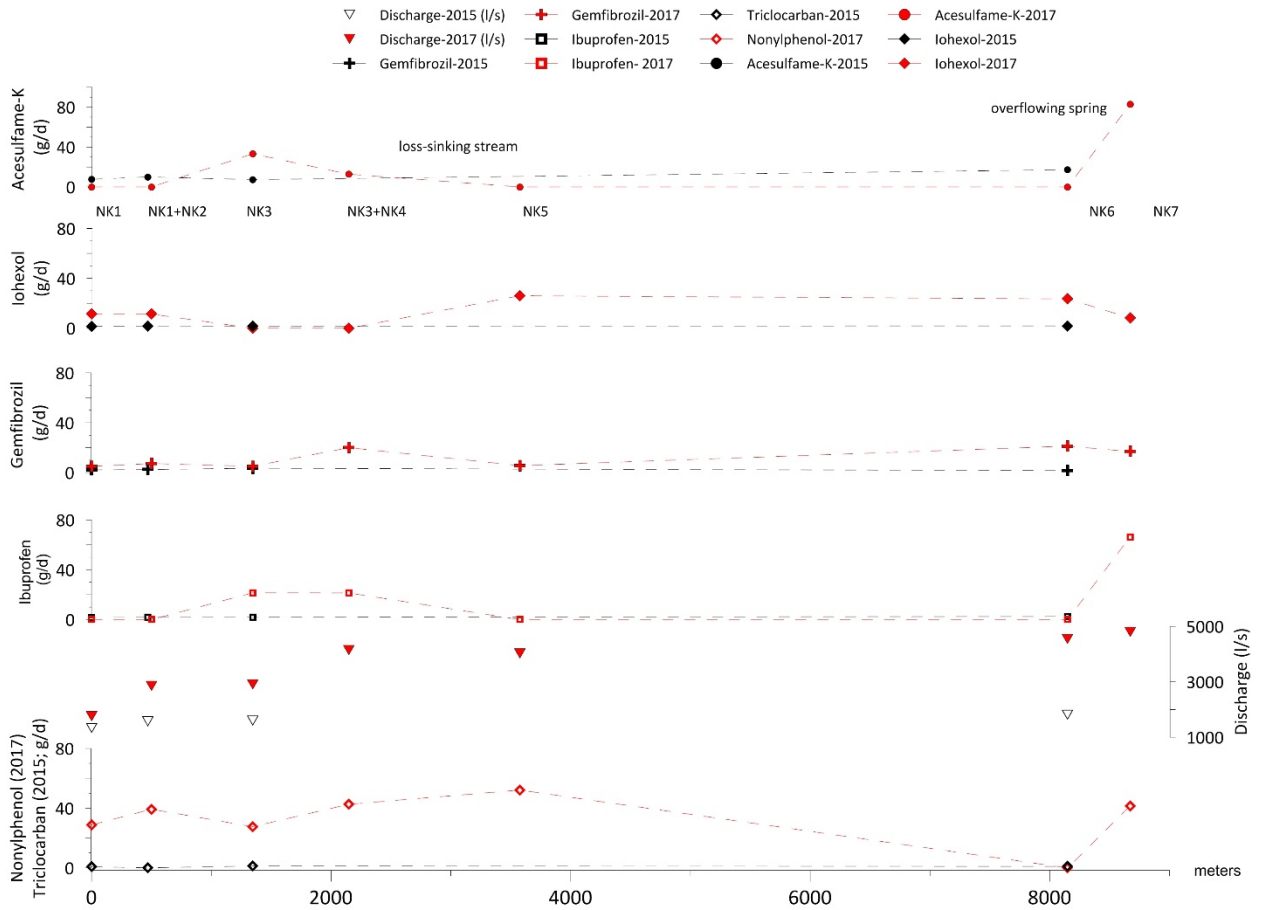


Figure 6-2. Comparison of variation of discharge and mass fluxes of micropollutants in both sampling campaigns

6.4 Insights into consumptions of persistent MPs

The number of inhabitants using GEM as a lipid regulator can be calculated for campaign 2 based on an average daily consumption (CDR_{MP}) of 1,200 mg (“drugs.com, Gemfibrozil”, 2017), with only 2% (R_{MP}) being excreted. For example, it is estimated that the total number of consumers of GEM as lipid regulator reaches 125 (campaign I) and 936 inhabitant in campaign II (with the additional input from RIII). NK4-0/NK4 lies downstream to a farm, a specific point source of pollution not due to human consumption. Poultry practices are believed to be the cause of the addition of GEM, and the hormones, ESD and EST. Pal et al., (2010), showed that major sources of estrogenic compounds to surface water

are not majorly discharged by WWTP, but also, directly by excretion of livestock. GEM is used to lower cholesterol in egg yolk and improve egg-shell quality (Mori et. al 1999). EST and ESD are used for the fattening of chickens (Umberger, 1975).

Additionally, if the average daily intake of ACE-K (CDR_{ACE-K}) is 1.22 mg/day (Subedi and Kannan, 2014) and ACE-K is released unchanged into the environment (Grice and Goldschmidt, 2000; Roberts et. al, 2000; Sims et al, 2000;), $R_{ACE-K}=1$); therefore the number of inhabitants on the three sub catchments consuming ACE-K products and releasing wastewater effluents onto the river catchment is estimated at 8280 (campaign I, excluding RIII) - 37,700 capita (campaign II mostly RIII). However it appears that ACE-K is not used as an artificial sweetener for dietary use only, but along with IBU in non-steroidal anti-inflammatory medicine.

6.5 Interaction between surface water and spring

Given the calculated mass loads, MPs such as ACE-K, IOX, and TRI appear to be present and persistent in the matrix of the spring and groundwater system. An important source of infiltration is the sinking stream after location NK3 that infiltrates into the Qachqouch spring. The River contributes only about 3% of the mass loads; higher percentage should be expected during flood periods. The daily mass loads of ACE-K in the River before NK5 ranges between 7.3 and 46 g/d. Therefore it is expected that about 0.2- 1.4 g/d infiltrate into the spring through fast flow pathways. The mass loads of ACE-K in the spring vary between 2.02 and 23.5 g/d outside flood periods ($Q > 3000 \text{ l/s}$). Therefore, the loads of persistent MPs in the sinking stream consist of about 1-6 % of the mass loads observed at the spring. The same calculations yield 1-17% for GEM. These percentages are related to the variation of loads in wastewater effluents along the river and the extent of dilution at the

spring. On the other hand, at the beginning of the hydrological year, flood flushing runoff could occur while most of the spring discharge originates only from base flow (<200 l/s), in the latter case, the River could contribute to up to 70 % of the mass loads present in the spring. Slow infiltration of surface water could also be implied from the lack of MPs with short half-lives (IBU, DIC, and CAF) in the spring, (Syed et. al 2011), due to their degradation. The persistence of some MPs (ACE-K) in groundwater could be explained by the diffuse infiltration of old stored wastewater through sewage sludge (Lapworth et al., 2012) that reaches the spring slowly after a considerable time thus prevailing during low flow. Another study done by Drewes (2009), shows that surface and groundwater interfaces could also transport MPs through lateral and vertical hydraulic exchange.

Therefore, with a continuous increasing inflow of untreated MPs in surface water into the GW aquifer of Qachqouch spring, it is assumed that the River will eventually lead to a more considerable input. In that case, continuous monitoring of concentrations and mass fluxes of these micropollutants in both spring and River will allow identifying intervals during which MPs' concentration may reach toxicity limits, especially with increasing urbanization on the catchment. A similar approach was used by Enseidl et al., (2010) to predict concentrations of MPs in a karst aquifer.

6.6 Origin and mass loads of the selected MPs

Both ASWs, as well as GEM are found in the spring during baseline (where no active recharge is occurring), during the events, and post events. This indicates that despite the significant dilution, the three MPs are found in the fissured matrix/epikarst at relatively high concentrations (e.g., SUC >100 ng/l), corresponding to daily loads of 3.0, 2.0 and 0.2 g of SUC, ACE-K, and GEM respectively.

Despite the presence of SUC and ACE-K in phreatic waters (as observed from the pre-event background concentrations), the mass of the four investigated MPs increased substantially during the inflow of fast infiltrated groundwater and flood waters. In the three events, varying percentages of flood waters (between 3.0 and 24% from the total volume discharged) were accompanied by varying mass loads of MPs. In the first and second event, the fast flow pathways were saturated with highly mineralized pre-event water that gets flushed away in the spring's first and second responses. The latter can explain the relatively low percentage of new water reaching the spring. As the system becomes more saturated with low mineralized event water, a higher volume of flood water infiltrates through fast flow pathways such as sinkholes and dolines to reach the spring in the third event. The depletion in stable isotopes (e.g., deuterium) observed with every spring response confirms that the origin of the fast flow is located on the dolines' plateau on highlands of the catchment between 1200 and 1500 m. In the third event, a significant enrichment in deuterium and heavy oxygen observed during the secondary turbidity peak, implies an infiltration of additional new waters from a lower recharge area on the catchment (800 m) corresponding to the river input via the sinking stream.

The correlation of turbidity and breakthrough of ASWs allows the identification of wastewater origin (hospital and domestic) and the mode of infiltration (River versus dolines). While SUC is arriving mostly through point source fast infiltration pathways, significant mass loads of ACE-K, GEM and IOX are also infiltrating along with surface water from a sinking stream along the Kalb River, which is very typical of karst landscapes. The lower loads of SUC in the river are due either to its absence in the wastewater effluent in the river, to SUC concentration falling below its relatively high detection limits (100 ng/l), or to mineralization of SUC in soils or river sediments (Labare and Alexander, 1993), decreasing

its concentration in the sinking stream. Sucralose was found in the wastewater effluent on the catchment area and in spring water (estimated from SUC mass fluxes in the spring; Table 5-5). Therefore its absence from the surface water catchment can be ruled out. As a matter of fact, it has been reported that SUC is characterized by a lower likelihood for detection (Kokotou and Thomaidis, 2013; Subedi and Kannan, 2014) especially in sludge material typical of non-treated wastewater.

The added ASWs' mass loads/event through direct rain infiltration correlate linearly; indicating that they have the same origin, infiltrating from point source wastewater (with a definite ratio of SUC to ACE-K), and rapid infiltration to the saturated zone (except for the infiltrated surface water). In all of the events, the persistence of ASWs, more specifically ACE-K in the phreatic zone, could also originate from slow continuous infiltration from the river into groundwater through bank filtrates, which is enhanced during high flow periods (Engelhardt et al, 2013). The correlation between masses of GEM and IOX may indicate a similar origin for the two MPs as well.

6.7 Correlation of MPs and in-situ parameters measured at the spring

Since the ASWs' mass fluxes and those of Cl correlate to a high extent, Cl (corrected for flow rate) could allow the quantification of the mass flux/concentrations of the two ASWs at the spring. Cl mass and TU fluxes correlate less with GEM and almost at no time with IOX; indicating a less conservative behavior of IOX with respect to the three other MPs. The short-term breakthrough of the contrast media is most probably related to sporadic point source hospital effluents and its limited release on the catchment.

The comparison of the normalized breakthrough curves with respect to peak concentration and transit time) for the first two events show that the breakthrough of

turbidity, ACE-K, SUC, and GEM are well synchronized. The slightly higher variance of ACE-K breakthrough curve with respect to that of SUC and turbidity could be reflective of a longer duration of breakthrough, potentially attributed to varying transport processes (e.g, dispersion). Moreover even if not detectable in the chemograph or hydrograph, an additional input of mass flux from a point source contamination such as the River (in the case of ACE-K) could also explain the tailing effect observed in events 1 and 2.

Studies have shown that ACE-K showed no retardation in porous aquifers with respect to Carbamazepine (Stempvoort et al., 2013) or karst aquifers with respect to CYC and uranine (Hillebrand et al., 2015). However, a higher sorption to suspended particulate matter of ACE –K was observed by Subedi and Kannan (2014). Nevertheless, since the breakthrough curve is resulting from convoluted multiple peaks of ASWs' mass fluxes, transport parameters such as dispersion cannot be calculated for each of the MPs.

IOX appears to be poorly synchronized with the turbidity flux breakthrough therefore, unlike ACE-K and SUC, TU and Cl could be considered less associated with the breakthrough of IOX, especially with the observed lag time. Finally, the secondary turbidity peak originating from the river input coincided solely with a breakthrough of ACE-K, GEM and IOX, showing that SUC is a poor indicator of infiltrated river water.

6.8 Suitability of the MPs as wastewater indicators

This study reveals that ACE-K proves to be a good wastewater indicator. Its breakthrough is concordant with the turbidity signals and the arrival of infiltrating wastewater into the spring from both surface water and fast infiltration pathways. Sucralose failed to be an indicator of wastewater from surface water effluents. On the other hand, GEM appears to be a suitable wastewater indicator, especially for transport of river water into groundwater.

However unlike SUC and ACE-K, it correlates less with Cl and TU. Finally, the breakthrough of IOX is relatively short at the spring with respect to the other investigated MPs, indicating a rather limited release in wastewater. Therefore it can be regarded as an indicator of hospital effluents for short term breakthrough events. The combination of easily monitored parameters at the spring such as Cl and TU can be used to predict concentrations and duration of breakthrough of wastewater indicators MPs (especially ACE-K and SUC), which is essential for contamination management purposes.

CHAPTER 7. CONCLUSION

The frequency of occurrence of selected MPs was detected based on two sampling campaigns undertaken under different flow conditions (2015 and 2017) on a surface water catchment connected to a karst spring. The study reveals that four MPs: ACE-K, IBU, GEM, and IOX are frequently detected and persistent in low flow and high flow in surface water in addition to the cleaning agents TRI and NON. They can be used as indicators of domestic wastewater effluents along river flanks as well as pollution from specific point sources such as poultry farms and hospitals.

Untreated wastewater effluents estimated with a mixing model consist of about 0.7–99% and 5.0–10% of pristine water inflowing from various tributaries in campaign 1 and campaign 2, respectively.

Additionally, an increase of MPs mass loads is observed between 2015 and 2017. The latter is explained by the presence of highly active tributaries and highly loaded wastewater during high flow or an increase in the consumption of micropollutants over a 2-year span.

The number of consumers of specific MPs such as GEM and ACE-K was calculated based on mass loads and daily consumption rates to have an insight into the consumption of these MPs in rural settings. ACE-K and IBU mass fluxes correlate very well, which indicates their similar origin and combined use in one specific medicine. The decrease of IBU occurrence with respect to ACE-K, observed during low flow, is related to the higher degradation rate of IBU in old stored wastewater with respect to a more persistent ACEK.

The concentrations observed in groundwater (spring and wells) cannot be fully associated with river infiltration; however, it is calculated that about 1–17% of MPs' masses (ACE-K and GEM) observed in the spring can be linked back to the sinking stream depending on the spring dilution and wastewater concentrations.

The concentrations of the two artificial sweeteners (SUC and ACE-K) along with a contrast media (IOX), and lipid regulator (GEM) were monitored following three consecutive rain events. Most of the investigated MPs are persistent in the matrix during low flow periods. They are further introduced with infiltrated flood waters through fast flow pathways e.g., dolines, which explain the observed peaks of MPs' despite the relative high dilution. An additional secondary peak of GEM, IOX, and ACE-K was observed in the third event, indicating rapid infiltration of wastewater from contaminated River water.

Given that a suitable wastewater indicator is defined by its persistence in groundwater storage and its particular origin (such as hospital waste for IOX), the four MPs ACE-K, SUC, GEM, and to a lesser extent IOX, can be envisaged as indicators of wastewater originating from various sources (autochthonous versus allochthonous sources). However SUC breakthrough curve fails to reflect the infiltration of contaminated river water into the spring, either because SUC falls below the detection limits or because of its controversial absence in surface water samples. Additionally, a good wastewater indicator is characterized by a high likelihood of detection because of its predominant usage on the catchment or high resolution of detection. The analytical limits of each of GEM, ACE-K, and IOX are below 10.0 ng/l, while that of SUC is 100 ng/l, thus decreasing its likelihood of detection unless present at relatively high concentrations (high mass fluxes). Nevertheless, SUC is to become a promising indicator for fast infiltrated groundwater given its increasing usage on the GW catchment area over other artificial sweeteners.

The MPs slightly varying transport behaviors, consumption loads, and potential origin, are reflected in their breakthrough's concentrations (peak concentrations) and duration at the spring. The mass flux of TU and Cl are strongly correlated with those of the two ASWs and to a lesser extent with GEM, while IOX appear to be less reliable because of its sporadic and short breakthrough. Additionally this correlation between ASWs and parameters that are easily measured in-situ at the spring can be used to predict the breakthrough of SUC and ACE-K as wastewater indicators and thus be reflective of the specific variable spring vulnerability. Finally, a long term monitoring of these selected MPs and parameters such as Chloride, Turbidity, or bacteriological contamination can help validate the results under varying flow periods.

CHAPTER

8. REFERENCES

- Andreozzi, R, Raffaele, M, Nicklas, P. (2003). Pharmaceuticals in STP effluents and their solar photodegradation in aquatic environment. *Chemosphere*. Volume 50, Issue 10, March 2003, Pages 1319-1330
- Andreozzi, R, Campanella, L, Frayse, B, Garric, J, Gonnella, A, Lo Giudice, R, Marotta, R, Pinto, G, Pollio, A. (2004). Effects of advanced oxidation processes (AOPs) on the toxicity of a mixture of pharmaceuticals. *Water Sci Technol* 50 (5): 23-28.
- Araujo, L., Villa, N., Camargo, N. (2009). Persistence of gemfibrozil, naproxen and mefenamic acid in natural waters. *Environ Chem Lett*. 9:13–18 DOI 10.1007/s10311-009-0239-5
- Ashton, K. (1966). The analysis of flow data from karst drainage systems. *Transactions of the Cave Research Group of Great Britain*, 7, 161-203.
- Atkinson, T., C., (1977). Diffuse flow and conduit flow in limestone terrain in Mendi. Hills, Somerset, England. *Journal of Hydrology*, 35: 93-100.
- Atkinson, T.C., Smith, D.I., Lavis, J.J. & Whiteaker, R.j. (1973). Experiments in tracing underground waters in limestones. *Journal of Hydrology*, 19, 323-349.
- Baedke, S.J., and Krothe, N.C., (2001). Derivation of effective hydraulic parameters of a karst aquifer from discharge hydrograph analysis. *Water Resources Research*, 37, no. 1:13-19.
- Bakalowicz, M. (2005). Karst groundwater: a challenge for new resources, *Hydrogeology Journal*, 13: 148-160.
- Bear, J. (1979). *Hydraulics of Groundwater*. McGraw-Hill Series in Water Resources and Environmental Engineering.
- Bendz D, Paxe´us N, Ginn T, Loge F (2005). Occurrence and fate of pharmaceutically active compounds in the environment, a case study: Ho¨je river in Sweden. *J Hazard Mater* 122:195–204.
- Booth, J, Boyland, E, (1970). The metabolism of nicotine into two optically active stereoisomers of nicotine-1'-oxide by animal tissues in vitro and by cigarette smokers. *Biochemical pharmacology*, 1970 - Elsevier Volume 19, Issue 3, Pages 733-742
- Bortolotti, A., Jiritano, L, Bonati M. (1985). Pharmacokinetics of paraxanthine, one of the primary metabolites of caffeine, in the rat. *Drug metabolism and disposition*. 13 (2) 227-231.
- Brosig, K., Geyer T., Subah, A., and Sauter, M. (2008). Travel time based approach for the assessment of vulnerability of karst groundwater: the transit time method. *Environmental geology*, 54, no 5:905-911.
- Brorström-Lundén, E., Svenson, A., Viktor, T., Woldegiorgis, A., Remberger, M., Kaj, L., Dye, C., Bjerke, A., Schlabach, M. NILU. (2008). Measurements of Sucralose in the Swedish Screening Program.
- Brown, M.C. & Ford, D.C. (1971). Quantitative tracer methods for investigations of karst hydrologic systems with special reference of the Maligne Basin area. *Trans. Cave Res. Group of Great Britain*, 13, 37-51.
- Brown, M.C., Wigley, T.M.L & Ford, D.C. (1969). Water budget studies in karst aquifers. *Journal of Hydrology*, 9, 113-116.
- Buerge, I, Poiger, T, Müller, M, and Buser, H. (2003). Caffeine, an Anthropogenic Marker for Wastewater Contamination of Surface Waters *Environ. Sci. Technol.*, 2003, 37 (4), pp 691–700.
- Buerge, I. J.; Buser, H.-R.; Kahle, M.; Müller, M. D.; Poiger, T. (2009). Ubiquitous occurrence of the artificial sweetener acesulfame in the aquatic environment: an ideal chemical marker of domestic wastewater in groundwater. *Environ. Sci. Technol.* 43 (12), 4381–4385.
- Butscher, C., and Huggenberger, P. (2009). Enhanced vulnerability assessment in karst areas by combining mapping with modelling approaches. *Science of the total environment*, 407, no. 3: 1153-1163.
- Canadian National Guidelines and Standards Office (2002). <http://www.ec.gc.ca/ese-ees/default.asp?lang=en&n=92f47c5d-1>
- Castronovo, S, Wick, A, Scheurer, M, Nödler, K, Schulz, M, Ternes, T. (2017). Biodegradation of the artificial sweetener acesulfame in biological wastewater treatment and sandfilters. *Water Research* Volume 110, Pages 342-353.
- Caviglioli, G, Valeria, P, Brunella, P, Cafaggi, S, Attilia, A, Gaetano, B (2002). Identification of degradation products of Ibuprofen arising from oxidative and thermal treatments. *Journal of Pharmaceutical and Biomedical Analysis*. Volume 30, Issue 3, Pages 499-509. [https://doi.org/10.1016/S0731-7085\(02\)00400-4](https://doi.org/10.1016/S0731-7085(02)00400-4)
- Civita, M. (2010). The combined approach when assessing and mapping groundwater vulnerability to contamination. *Journal of Water Resource and Protection*, 2:14-28.
- Clara, M., Strenn, B., Kreuzinger, N. (2004). Carbamazepine as a possible anthropogenic marker in the aquatic environment: investigations on the behaviour of Carbamazepine in wastewater treatment and during groundwater infiltration. *Water Res.* 38 (4), 947–954.
- Climent, L, Collado, N, Buttiglieri, G, Gros, M, Rodriguez-Roda, I, Rodriguez-Mozaz, S, Barceló, D. (2012). Comprehensive study of ibuprofen and its metabolites in activated sludge batch experiments and aquatic environment. *Science of The Total Environment*. Volume 438, 1 November 2012, Pages 404-413. <https://doi.org/10.1016/j.scitotenv.2012.08.073>
- COST: Action 620, (2003). Vulnerability and risk mapping for the protection of carbonate (karst) aquifers, European Commission, Directorate-General for Research, Report EUR 20912, Luxemburg.
- Criss, R., E. (1999). Principles of stable isotope distribution. New York: Oxford University Press.
- Dansgard, W. (1964). Stable isotopes in precipitation. *Tellus*, 16, 436-468.
- Daughton C, Ternes T. (1999). Pharmaceuticals and personal care products in the environment: agents of subtle change? *Environmental Health, Perspect* 107 (suppl 6):907-938.

- Dewaide, L., Collon, P., Poulain, A., Rochez, G., Hallet, V. (2018). Double-peaked breakthrough curves as a consequence of solute transport through underground lakes: a case study of the Furfooz karst system, Belgium. *Hydrogeology Journal*. Volume 26, Issue 2, pp 641–650
- Doummar, J., Margane, A., Geyer, T., Sauter, M. (2010a). Artificial Tracer Tests. Special Report No.1 of Technical Cooperation Project “Protection of Jeita Spring”.
- Doummar, J., Margane, A., Geyer, T., Sauter, M. (2010b). Artificial Tracer Tests. Special Report No.2 of Technical Cooperation Project “Protection of Jeita Spring”.
- Doummar, J., Sauter, M., and Geyer, T. (2012). Simulation of flow processes in a large scale karst system with an integrated catchment model (Mike She) – Identification of relevant parameters influencing spring discharge. *Journal of Hydrology*. 426-427: 112-123.
- Doummar, J., Geyer, T., Baierl, M., Nödler, K., Licha, T., and Sauter, M. (2014). Carbamazepine breakthrough as indicator for specific vulnerability of karst springs: Application on the Jeita spring, Lebanon. *Applied Geochemistry*. 47, 150–156.
- Doummar, J., & Margane, A., & Geyer, T., & Sauter, M. (2018). Assessment of key transport parameters in a karst system under different dynamic conditions based on tracer experiments: the Jeita karst system, Lebanon. *Hydrogeology Journal*. 10.1007/s10040-018-1754-
- Drugs.com (2017).<https://www.drugs.com/pro/gemfibrozil.html>
- Drugbank.com (October 2, 2017). <http://www.drugbank.ca/drugs/DB01362>.
- Dubois, E. (2017). Analysis of high resolution spring hydrographs and climatic data: application on the Qachqouch spring (Lebanon). emecine.medscape.com
- Fetter, C. w. (1999). *Applied Hydrogeology*, fourth international edition.
- Field, M.S. (1990). Transport of chemical contaminants in karst terranes: Outline and Summary. In selected papers on Hydrogeology, edited by E. S. Sharp and J.M. Sharp, Jr, 1:17-27.
- Field M., S., & Pinsky, P., F. (2000). A two region nonequilibrium model for solute transport in solution conduits in karstic aquifers. *J. Contam. Hydrol.*, 44,329-351.
- Food and Drug Administration (FDA). (2006). <https://www.fda.gov/Food/default.htm>
- Ford, D.C., Williams, P.W., 1989. *Karst Geomorphology and Hydrology*. Unwin Hyman, London, 601 pp.
- Ford, D., Williams, P. (2007). *Karst Hydrogeology and Geomorphology*. Wiley. New York.
- Foster, S., S., D. (1987). Fundamental concepts in aquifer vulnerability, pollution risk and protection strategy. In: van Duijnboden W, van Waegeningh HG (eds). *Vulnerability of soil and groundwater to pollutants*. Proceedings and information n.38, TNO committee on hydrological research, The Hague: 69-86.
- Fox J. (2008). Companion to Applied Regression. R package version 1.2 9. Available: <http://cran.r-project.org/web/packages/car>.
- Galmier, MJ, Bouchon, B, Madelmont, JC, Mercier, F, Pilotaz, F, Lartigue, C. (2005). Identification of degradation products of diclofenac by electrospray ion trap mass spectrometry. *Journal of Pharmaceutical and Biomedical Analysis*. Volume 38, Issue 4, 15 July 2005, Pages 790-796.
- Gasser, G., rona, M., Voloshenko, A., Shelkov, R., Tal, N., Pankratov, I., Elhanany, S., Lev, O. (2010). Quantitative evaluation of tracers for quantification of wastewater contamination of potable water sources. *Environmental Science & Technology*, 44 (10), pp. 391903925.
- Geyer, T., Birk, S., Licha, T., Liedl, R., and Sauter, M. (2007). Multi-tracer test approach to characterize reactive transport in karst aquifers. *Ground Water*. 45, no. 1: 36-45.
- Goldscheider, N. (2002). *Hydrogeology and vulnerability of karst systems: examples from the Northern Alps and Swabian Alb*. Ph.D. Thesis, Schr. Angew. Geol Karlsruhe, 236pp.
- Goldscheider, N., and Drew, D. (2007). *Methods in Karst Hydrogeology*. International Association of Hydrogeologists.
- Goldscheider N, Meiman J, PronkM, Smart C (2008) Tracer tests in karsthydrogeology and speleology. *Int J Speleol* 37(1):27–40.
- Göppert, N., & Goldscheider, N. (2008). Solute and colloid transport in karst conduits under low- and high-flow conditions *Ground Water* 46:1. 61-68
- Gozlan, I, Rotstein, A, Avisar, D. (2013). Amoxicillin-degradation products formed under controlled environmental conditions: Identification and determination in the aquatic environment. *Chemosphere* Volume 91, Issue 7, Pages 985-992
- Greskowiak, J, Gwo, J, Jacques, D, Yin, J, Mayer, U. (2015). A benchmark for multi-rate surface complexation and 1D dual-domain multi-component reactive transport of U(VI).
- Grice, H., C., Goldsmith, L., A. (2000). Sucralose—an overview of the toxicity data. *Food Chem. Toxicol.*, 38, pp. S1-S36.
- Guerreiro, S, Toulorge, D, Hirsch, E, Marien, M, Sokoloff, P and Patrick P. Michel, P. (2008). Paraxanthine, the Primary Metabolite of Caffeine Provides Protection against Dopaminergic Cell Death via Stimulation of Ryanodine Receptor Channels. *Molecular Pharmacology Fast Forward*. DOI: 10.1124/mol.108.048207
- Gulley, J, Walthard, P, Martin, J, Banwell, A. (2012). Conduit roughness and dye-trace breakthrough curves: why slow velocity and high dispersivity may not reflect flow in distributed systems. *Journal Of glaciology*. Volume 58, Issue 211. pp. 915-925. <https://doi.org/10.3189/2012JG11J115>. Published online: 08 September 2017
- Hauns M, Jeannin P-Y (1998) Tracer transport in underground rivers in karst: tailing effects and channel geometry. *Bull Hydrogéol* 16:123–142
- Hauns M, Jeannin P-Y, Atteia O (2001) Dispersion, retardation and scale effect in tracer breakthrough curves in karst conduits. *J Hydrol*241(3–4):177–193
- Hahne, K. (2011). Geological Map, Tectonics and Karstification in the Groundwater Contribution Zone of Jeita Spring supported by Remote Sensing - Technical Report 4 prepared by TC - Project “Protection of Jeita Spring”
- Halling-Sørensen, B., Nors Nielsen, S., Lanzky, P. F., Ingerslev, F., Holten Lützhøft, H., C., Jørgensen S., E. (1998). Occurrence, fate and effects of pharmaceutical substances in the environment-a review. *Chemosphere*. Jan;36(2):357-93.
- Halme, L, von Smitten, E & Linden, H. Increased Urinary Excretion of Iohexol after Enteral Administration in Patients

- with Ileal Crohn's Disease. *Journal of Acta Radiologica* Volume 34, 1993 - Issue 3, Pages 237-214
- Hamdan, A. (2018). Estimation of transit times in karst aquifers using environmental tracers (tritium, helium, chlorofluocarbons, and sulfur hexafluoride): application on Jeita aquifer system-Lebanon. Master Thesis, American University of Beirut, Lebanon
- Heithecker R. Aedo A.-R., Landgren B.M, Cekan S.Z., (1991). Plasma Estriol Levels after Intramuscular Injection of Estriol and Two of Its Esters. *Hormone research in pediatrics*. 1991;35:234–238
- Higuchi, A., Kohji, T., Shinji, I., Harumi, S., Kazue, Y., Keiko, T., Naoko, A., Keiko, U., Youko, S., Masahide, N., Masaharu, K., Katsutoshi, T., Atsushu, N., Hidekazu, S., Takehiro, T. (2004). Activities of Injection Waste Management Committee and Effect On induction of Intermediate Processing Device. *Environmental Injections* 19 (3), 415-420, 2004.
- Hillebrand, O., Nödler, K., Licha, T., Sauter, M., & Geyer, T. (2011). Caffeine as an indicator for the quantification of untreated wastewater in karst systems. *Water research*. 46. 395-402. 10.1016/j.watres.2011.11.003.
- Hillebrand, O. (2014). Fate of organic micropollutants in a karst aquifer system - Implications for sustainable raw water management. <http://ediss.uni-goettingen.de/handle/11858/00-1735-0000-0022-5F58-3?locale-attribute=de>.
- Hoque, M., Cloutier, F., Arcieri, C., McInnes, M., Sultana, T., Murray, C., Vanrolleghem, A., Metcalfe, C. (2014). Removal of selected pharmaceuticals, personal care products and artificial sweeteners in an aerated sewage lagoon. *Science of the Total Environment*, Volume 48, Pages 801-812
- Jarvis, MJ., Russell, MA, Benowitz, NL, and Feyerabend, C. (1988). Elimination of cotinine from body fluids: implications for noninvasive measurement of tobacco smoke exposure. *American Journal of Public Health (AJPH)*
- Jeannin, P.,Y., Cornaton, F., Zwahlen, F., and Perrochet, P., (2001). 7th conference on limestone hydrology and fissured media memoires hors serie, (Universite de France-Comte, Besancon), VULK a tool for intrinsic vulnerability assessment and validation, eds Zwahlen F., Murdy J. 13:185-188.
- Kaas, W. (1998). Tracing technique in geohydrology. Rotterdam, Brookfield: Balkema, 581 p.
- Keller, S. E., J. M. Weiss, S. J. Schleifer, N. E. Miller and M. Stein. (1981). Suppression of immunity of stress: Effect of a graded series of stressor on lymphocyte stimulation in the rat. *Science* 213:1397.
- Kilpatrick F. A. (1993). Techniques of water resources investigations of the United States Geological Survey. USGS, chapter A20.
- Király, L. (2002). Karstification and Groundwater Flow. In: Proceedings of the Conference on Evolution of Karst: From Prekarst to Cessation. Postojna-Ljubljana, 155-190.
- Königer, P; Margane, A. (2014). Stable Isotope Investigations in the Jeita Spring catchment. Bundesministerium für wirtschaftliche Zusammenarbeit und Entwicklung, BMZ
- Kormos, J., Schulz, M., and Ternes, T. (2011). Occurrence of Iodinated X-ray Contrast Media and Their Biotransformation Products in the Urban Water Cycle. *Environ. Sci. Technol.*, 45, 8723–8732.
- Kuehl, G. Bigler, J. Potter, J. and Lampe, J. (2006). Glucuronidation of the aspirin metabolite salicylic acid by expressed udp-glucuronosyltransferases and human liver microsomes. *Drug Metabolism and Disposition* 34 (2) 199-202; DOI: <https://doi.org/10.1124/dmd.105.005652>
- Kümmerer, K. (2009). The presence of pharmaceuticals in the environment due to human use, present knowledge and future challenges *J Environ Manage*. 90 pp. 2354–2366.
- Labare, M.P, and Lexand, M. (1992). Biodegradation of Sucralose, a Chlorinated Carbohydrate, In Samples of Natural Environments. *Environmental Toxicology and Chemistry* Vol 12, pp 797 804.
- Lange J, Greenbaum N, Husary S, Ghanem M, Leibundgut C, Schick AP. (2003). Runoff generation from successive simulated rainfalls on a rocky, semi-arid, Mediterranean hillslope. *Hydrological Processes* 17(2): 279–296.
- Lange J, Greenbaum N, Husary S, Timmer JG, Leibundgut C, Schick AP. (2003) b. Tracers for runoff generation studies in a Mediterranean region: comparison of different scales. In *Hydrology of Mediterranean and Semiarid Regions*, Servat E, Najem W, Leduc C, Shakeel A (eds), IAHS Publication No. 278. IAHS Press: Wallingford; 117–123.
- Latch, D, Stender B, Packer, J, Arnold, W[†], and McNeill, K. (2003). Photochemical Fate of Pharmaceuticals in the Environment: Cimetidine and Ranitidine. *Environ. Sci. Technol*, 37, 15, 3342-3350
- Leibundgut C., Maloszewski P., & Külls C. (2009) – Tracers in hydrology. Wiley-Blackwell, Sussex.
- Lim, F., Y., Ong, S., L., and Hu, J. (2017). Recent Advances in the Use of Chemical Markers for Tracing Wastewater Contamination in Aquatic Environment: A Review. *Water*, 9(2), 143; doi:10.3390/w9020143.
- Lin, A. Reinhard, M. (2009). Photodegradation of common environmental pharmaceuticals and estrogens in river water. *Environmental Chemistry*. Volume24, Issue6. Pages 1303-1309
- Liu, QT, and Williams, H. (2007). Kinetics and Degradation Products for Direct Photolysis of β -Blockers in Water. *Environ. Sci. Technol.*, 2007, 41 (3), pp 803–810 DOI: 10.1021/es0616130
- Liu, Y., Blowes, D., Groza, L., Sabourin, M. J., and Ptacek, C., J. (2014). Acesulfame-K and pharmaceuticals as co-tracers of municipal wastewater in a receiving river. *Environ. Sci.: Processes Impacts*, 16, 2789.
- Loos, R., Gawlik, B. M., Boettcher, K., Locoro, G., Contini, S., Bidoglio, G. (2009). Sucralose screening in European surface waters using a solid-phase extraction-liquid chromatography-triple quadrupole mass spectrometry method. *J. Chromatogr., A*, 1216 (7), 1126–1131.
- Mao, Z, Zheng, X, Zhang, Y,X, Li, Y and Wang, W. (2012). Occurrence and Biodegradation of Nonylphenol in the Environment. *INT. J. MOL. SCI.* 2012, 13(1), 491 505; <https://doi.org/10.3390/ijms13010491>
- Massei N, Wang HQ, Field MS, Dupont JP, Bakalowicz M, Rodet J. (2006). Interpreting tracer breakthrough tailing in a conduit-dominated karst aquifer. *Hydrogeol J* 14(6):849–858
- Margat, J. (1968). Contamination vulnerability mapping of groundwater, Bureau de recherches géologiques et minières, Orleans.
- Margane, A., Schuler, P., Koeniger, P., Raad, R., Abi Rizk, J., Stoeckl, L. (2013). Hydrogeology of the Groundwater Contribution Zone of Jeita Spring. - Technical Report No.5 of Technical Cooperation Project "Protection of Jeita Spring".
- Mawhinney, D. B., Young, R. B., Vanderford, B. J., Borch, T., Snyder, S. A. (2011). Artificial sweetener sucralose in U.S.

- drinking water systems. *Environ. Sci. Technol.* 45 (20), 8716–8722
- Mead, R., Morgan, J., Avery Jr., B Robert J., Kieber, R., Kirk, A., Skrabal, S., Joan D. Willey, J. (2009). Occurrence of the artificial sweetener sucralose in coastal and marine waters of the United States.
- Morales, T., Fdez de Valderram I., Uriate, J., A., Antigüedad, I., and Olazar, M. (2007). Predicting travel time and transport characterization in karst conduits by analyzing tracer breakthrough curves. *Journal of Hydrology*, 334: 183-198.
- Morales, T, Zhang, W, Gao, B, Lion, L, Bisogni, J, McDonough, B, Steenhuis, T. (2010). Impact of dissolved organic matter on colloid transport in the vadose zone: deterministic approximation of transport deposition coefficient from polymer coating characteristics. *Water Res.*, 45(4), 1691-1701
- Morales T, Uriarte JA, Olazar M, Antigüedad I, Angulo B. (2010) Solute transport modelling in karst conduits with slow zones during different hydrologic conditions. *J Hydrol* 390:182–189
- Mumford, G. K. Benowitz, N. L. Evans, S. M. Kaminski, B. J. Preston, K. L. Sannerud, C. A. Silverman, K. Griffiths, R. R. (1996). Absorption rate of methylxanthines following capsules, cola and chocolate. *European Journal of Clinical Pharmacology*. Volume 51, Issue 3–4, pp 319–325
- Nabuurs, M, van der Molen, E, de Graaf, G, Jager, L, (1990). Clinical Signs and Performance of Pigs Treated with Different Doses of Carbadox, Cyadox and Olaquinox. *Journal of transboundary and emerging diseases*. <https://doi.org/10.1111/j.1439-0442.1990.tb00877.x> Volume 37, Issue 1-10 Pages 68-76.
- Nader, F.H., Swennen R., and Ellam, R.M. (2007). Field geometry, petrography and geochemistry of a dolomitization front (Late Jurassic, central Lebanon). *Sedimentology*, 54: 1093-1119.
- Neukum, C., Hotzl, H., and Himmelsbach, T. (2008). Validation of Vulnerability mapping methods by field investigations and numerical modelling. *Hydrogeology Journal*, 16:641-658.
- Nicod, J. (1971). Quelques remarques sur la dissolution des dolomies. *Bulletin de l'Association de géographes français* 48, 247–261.
- Nödler, K., Tsakiri, M., Aloupi, M., Gatidou, G., Stasinakis, A., S., Licha, T. (2016). Evaluation of polar organic micropollutants as indicators for wastewater-related coastal water quality impairment. *Environmental Pollution* Volume 211, Pages 282-290.
- Novack, L, And Brodie, B (1950). Quinoline and its transformation products found in urine. *The Journal of Biological Chemistry* 187, 787-792.
- O'Neil, J., R. (1986b). Terminology and standards. *Reviews of mineralogy*, 16, 561-570.
- Ogilvie, B Donglu Zhang, D, Li, W, Rodrigues, D, Gipson, A, Holsapple, J, Toren, P, and Parkinson, A. Glucuronidation converts gemfibrozil to a potent, metabolism-dependent inhibitor of CYP2C8: Implications for drug-drug interactions. *Drug Metabolism and Disposition* January 2006, 34 (1) 191-197; DOI: <https://doi.org/10.1124/dmd.105.007633>
- Oppenheimer, J., Eaton, A., Badruzzaman, M., Haghani, A. W., Jacangelo, J., G. (2011). Occurrence and suitability of sucralose as an indicator compound of wastewater loading to surface waters in urbanized regions. *Water Res.* 45 (13), 4019–4027.
- Perkola, N., Sainio, P. H.-J., Stan, T., Heberer, M. Linkerhägner. (2014). *Environmental Pollution*. 184, pp. 391-396.
- Perrin, J, PY Jeannin, PY, Zwahlen Y. (2003). Epikarst storage in a karst aquifer: a conceptual model based on isotopic data, Milandre test site, Switzerland. *Journal of hydrology*. Volume 279, Issues 1–4, Pages 106-124
- Polemio, Dragone, & Limoni, P. (2009). Monitoring and methods to analyze the groundwater quality degradation risk in coastal karstic aquifers (Apulia, southern Italy). *Environmental Geology*, 58(2), 299-312. 10. 1007/s00254-008-1582-8.
- Pronk M., Goldscheider N., Zopfi J. (2006). Dynamics and interaction of organic carbon, turbidity and bacteria in a karst aquifer system. *Hydrogeol. J.* 14, 473–484 10.1007/s10040-005-0454-5.
- Putschew, A., Wischnack, S., Jekel, M. (2000). Occurrence of triiodinated X-ray contrast agents in the aquatic environment. *Sci. Total Environ.*, 255 (1), 129–134.
- Putschew, A., Schittko, S., Jekel, M. (2001). Quantification of triiodinated benzene derivatives and X-ray contrast media in water samples by liquid chromatography-electrospray tandem mass spectrometry. *J. Chromatogr. A* 930 (1–2) (2001) 127–134, doi:[http://dx.doi.org/10.1016/S0021-9673\(01\)01186-4](http://dx.doi.org/10.1016/S0021-9673(01)01186-4). 11681570.
- Reeves, PR, McAinsh, J, McIntosh, D, Winrow, MJ. (1978). Metabolism of atenolol in man *Xenobiotica* Volume 8, 1978 - Issue 5
- Reh, R., Licha, T., Geyer, T., Nödler, K., Sauter, M. (2013). Occurrence and spatial distribution of organic micro-pollutants in a complex hydrogeological karst system during low flow and high flow periods, results of a two-year study. *Science of the Total Environment* 443, 438–445.
- Roberts, A., Renwick, A.G., Sims, J., Snodin D, J. (2000). Sucralose metabolism and pharmacokinetics in man. *Food and Chemical Toxicology*, 38 (Suppl. 2), pp. S31-S41.
- Robertson, D., Van Stempvoort, D., K., Solomon, J., Homewood, S., Brown, J., Spoelstra, S., Schiff. L. (2013). Persistence of artificial sweeteners in a 15-year-old septic system plume. *Journal of Hydrology* Volume 477, Pages 43-54.
- Saint-Hilaire, D, Jans, U. (2013). Reactions of three halogenated organophosphorus flame retardants with reduced sulfur species. *Chemosphere*. Volume 93, Issue 9, November 2013, Pages 2033-2039
- Sanderson, H., Johnson, D., Wilson, C., Brain, R., Solomon, K. (2003). Probabilistic hazard assessment of environmentally occurring pharmaceuticals toxicity to fish, daphnias and algae by ECOSAR screening. *Toxicol Lett* 144:383–395.
- Sang, Z., Jiang, Y., Tsoi, Y., Leung, K. (2014). Evaluating the environmental impact of artificial sweeteners: A study of their distributions, photodegradation and toxicities
- Sauerhoff, Braun, W, Blau, G, Gehring, G. (1977). The fate of 2, 4 dichlorophenoxyacetic acid (2, 4-D) following oral administration to man. *Toxicology* Volume 8, Issue 1, Pages 3-11.
- Sauter, M. (1992). Quantification and forecasting of regional groundwater flow and transport in karst aquifer (Gallusquelle, Malm, SW. Germany). *Tubinger Geowissenschaftliche Arbeiten*, C13, 150 pp.
- Sauter, M. (1997). Differentiation of fast and slow flow components in a karst aquifer using oxygen 18 signature-data

- analysis and modelling. In Kranjc, A. (ed). *Tracer Hydrology* 97, Balkema: 435-441.
- Schebb, N. H. Franze, B. Maul, R. Ranganathan, A. and Hammock, B. D. (2012). In Vitro Glucuronidation of the Antibacterial Triclocarban and Its Oxidative Metabolites. *Drug Metabolism and Disposition*, 40 (1) 25-31; DOI: <https://doi.org/10.1124/dmd.111.042283>.
- Scheytt, T., J., Mersmann, P., Heberer, T. (2006). Mobility of pharmaceuticals carbamazepine, diclofenac, ibuprofen, and propyphenazone in miscible-displacement experiments. *J. Contam. Hydrol.* 83, 53e69.
- Scheurer, M., Brauch, H.-J., Lange, F. T. (2009). Analysis and occurrence of seven artificial sweeteners in German wastewater and surface water and in soil aquifer treatment (SAT). *Anal. Bioanal. Chem.* 394 (6), 1585–1594.
- Schlulz, H. D. (1998). Evaluation and interpretation of tracing tests.
- Schnegg, P. A. (2002). An inexpensive field fluorometer for hydrogeological tracer tests with three tracers and turbidity measurement. XXXII IAH and ALHSUD Congress Groundwater & Human Development. Bocanegra, E., Martinez, D., Massone, H. (eds) ISBN 987-544-063-9.
- Schröder, H, Campbell, D. (1972). Absorption, metabolism, and excretion of salicylazosulfapyridine in man. *Clinical pharmacology and therapeutics Journal*. Volume 13, Issue 4, Pages 539-551
- Schwarzenbach, R. P., Escher B., I., Fenner, K., Hofstetter, T., B., Johnson, C., A., von Gunten, U., Wehrli, B. (2006). The challenge of micropollutants in aquatic systems. *Science* 313, 1072–1077.
- Seiler, K.-P., Maloszewski, P. & Behrens, H. (1989). Hydrodynamic dispersion in karstified limestone and dolomites in Upper Jura of Franconian Alb, FRG. *Journal of Hydrology*, 108; 235-247.
- Sidney S. Walkenstein, S. Knebel, C. MacMullen, J, and Seifter, J. (1958). The excretion and distribution of Meprobamate and its metabolites. *Journal of Pharmacology and Experimental Therapeutics* August 1958, 123 (4) 254-258
- Sims, J., Roberts, A., Daniel, J.W., Renwick, A.G. (2000). The metabolic fate of sucralose in rats. *Food and Chemical Toxicology*. Volume 38, Supplement 2, Pages 115-121.
- Smart, C. (1988). Artificial tracer techniques for determination of the structure of conduit aquifers. *Ground Water*, 26, 445-453.
- Snow, D. H, Baxter, P, Whiting, B. (1981). The pharmacokinetics of meclofenamic acid in the horse. *Journal of veterinary pharmacology and therapeutics* Volume 4, Issue 2. Pages 147-156.
- Soares, A., Guieysse, B., Jefferson, B., Cartmell, E., & Lester, J.N. (2008). Nonylphenol in the Environment: A Critical Review on Occurrence, Fate, Toxicity and Treatment in Wastewaters. *Environment international*. 34. 1033-49. [10.1016/j.envint.2008.01.004](https://doi.org/10.1016/j.envint.2008.01.004).
- Spoolstra J., Schiff S., L., Brown S., J. (2013). Artificial Sweeteners in a Large Canadian River Reflect Human Consumption in the Watershed. Taken from: *PLoS ONE* 8(12): e82706. doi:10.1371/journal.pone.0082706.
- Stan, H., J., and Linkerhagner M. (1992). "Identifizierung von 2-(4-Chlorphenoxy)-2methyl-propionsäure im Grundwasser mittels Kapillar-Gaschromatographie mit Atomemissionsdetektion und Massenpektrometrie". *Vom Wasser* 79: 75-88.
- Stan, H., J, Heberer, T., Linkerhäger M. (1994). "Occurrence of chlorofibric acid in the aquatic system: Is their therapeutic use responsible for the loads found in surface, ground- and drinking water?". *Vom Wasser*, 83: 57-68.
- Stanczyk, F, Archer, D., (2013). Ethinyl estradiol and 17 β -estradiol in combined oral contraceptives: pharmacokinetics, pharmacodynamics and risk assessment. *Contraception Journal*. Volume 87, Issue 6, June 2013, Pages 706 727. <https://doi.org/10.1016/j.contraception.2012.12.011>
- Stempvoort, D., Roy, J., W., Brown, S., J., Bickerton, G. (2011). Artificial sweeteners as potential tracers in groundwater in urban environments. *Journal of Hydrology*. Volume 401, Issues 1–2, 20, Pages 126-133.
- Stempvoort, D., Roy, J., W., Grabuski, J., Brown, S., J., Bickerton, G., Sverko, E. (2013). An artificial sweetener and pharmaceutical compounds as co-tracers of urban wastewater in groundwater. *Science of the Total Environment*. Volumes 461–462, Pages 348-359.
- Subedi, B, Kannan, K. (2014). Fate of artificial sweeteners in wastewater treatment plants in New York State, USA. *Environmental science & technology*. 48 (23), pp 13668–13674. DOI: [10.1021/es504769c](https://doi.org/10.1021/es504769c)
- Ternes, T, A., Hirsch, R. (2000). Occurrence and behavior of X-ray contrast media in sewage facilities and the aquatic environment, *Environ. Sci. Technol.* 34 (13), 2741–2748, doi:<http://dx.doi.org/10.1021/es991118m>.
- Ting W. Nigel, C.Graham, JD, WeiChu, W. (2010). Degradation of iopromide by combined UV irradiation and peroxydisulfate. *Journal of Hazardous Materials*. Volume 181, Issues 1–3, Pages 508-513.
- Toride, N., Leij, F. J and van Genuchten. (1999). The CXTFIT code for estimating transport parameters from laboratory or field tracer experiments. *US Salinity Laboratory, USDA, ARS, Riverside, CA.toxnet.nlm.nih.gov*
- Torres, C.I., Ramakrishna, S., Chiu, C.-A., Nelson, K.G., Westerhoff, P., Krajmalnik-Brown, R. (2011). Fate of sucralose during wastewater treatment *Environ. Eng. Sci.*, 28 (5), pp. 325-331.
- Tran, N.H, Nguyen, V.T, Uruse, T. (2014). Ngo, H.H. Role of nitrification in the biodegradation of selected artificial sweetening agents in biological wastewater treatment process. *Bioresource Technology* 161, 40–46.
- Vias, J., M., Andreo, B., Perles, M., J., Carrasco, F., Vadillo, I., and Jimenez, P. (2006). Proposed method for groundwater vulnerability mapping in carbonate (karstic) aquifers: the COP method application in two pilot site in Southern Spain, *Hydrogeology Journal*, 14: 912-925.
- Wachniew, P. (2015). Environmental tracers as a tool in groundwater vulnerability assessment. *Acque Sotterranee - Italian Journal of Groundwater* (2015) - AS13059: 019 – 025.
- Weiss M, Gvirtzman H. 2006. Estimating ground water recharge using flow models of perched karstic aquifers. *Ground Water* 45(6): 761–773.
- Werner, A, Hotzl, H, Kaas, W. (1997). The Interpretation of a high water tracer test in the Danube-Aach-System (Western Swabian Alb, Germany). 6th conference on limestone hydrology and fissured media, La Chaux-de-Fonds, Switzerland, *Limestone Hydrology and Fissured Media, La Chaux-de-Fonds, Switzerland*, 187-190.
- Werner, A., H. Hotzl & Kaas, W. (1997b). The interpretation of a high water tracer test in the Daune-Aach-System with

analytical models. Proc. 5th Symp. On Karst Waters & Environmental Impacts 1995, p 153-160. Rotterdam: Balkema.

White, W.B., and White, E.L., (1998). Geology, in A Guide to Speleological Literature, Northup, D.E., Mobley, E.D., Ingham, K.L., and Mixon, W.W., eds., p. 40-41.

White, W.B., (1988). Geomorphology and Hydrology of Karst Terrains. Oxford Univ. Press, New York, 464 pp.

White WB. (2002). Karst hydrology: recent developments and open questions. Eng Geol 65:85-105

Williams, P. W. (1983). The role of the subcutaneous zone in karst hydrology. Journal of hydrology, 61: 45-67.

Wolf, L., Zwiener, C., Zemann, M. (2012). Tracking artificial sweeteners and pharmaceuticals introduced into urban groundwater by leaking sewer networks. Sci. Total Environ., 430, pp. 8-19.

Wood, S., G., John, B., A., Hawkins, D., R. (2000). The pharmacokinetics and metabolism of sucralose in the dog Food and Chemical Toxicology, 38 (Suppl. 2), pp. S99-S106.

Ying, G, Yu, X, Kookana, R. (2007). Biological degradation of triclocarban and triclosan in a soil under aerobic and anaerobic conditions and comparison with environmental fate modelling. Environmental Pollution. Volume 150, Issue 3, December 2007, Pages 300-305

Zuccaato E., Chiabrando C., Castiglioni S., Calamari D., Bagnati R., Schiarea S., Fanelli R. (2005). Cocaine in surface waters: a new evidence-based tool to monitor community drug abuse. Environ. Health 4, 14. (doi:10.1186/1476-069X-4-14).